The Vector Paradigm in Modern NMR Spectroscopy:

II. Description of Pulse Sequences in Coupled Two-Spin Systems.

William M. Westler

Keywords: NMR, pulse sequence, product operator, scalar coupling

National Magnetic Resonance Facility at Madison

Department of Biochemistry

433 Babcock Drive

University of Wisconsin-Madison, Madison WI 53706

Telephone: 608-263-9599

Fax: 608-263-1722

E-Mail: milo@nmrfam.wisc.edu

A popular approach to the description of NMR pulse sequences comes from a simple vector model, in which the motion of the spins subjected to RF pulses and chemical shifts is described by the rotations of a classical vector in three-dimensional space. The major weakness in this model is that spin systems that contain scalar coupling are not adequately described. The ultimate description of NMR experiments is through the application of density matrix theory. However, this treatment is not very transparent (or understandable to the uninitiated) and does not lead easily to an intuitive feel for the behavior of spins in NMR experiments. In 1983, several groups independently introduced the product operator formalism as a simplification of density matrix theory(##). In this treatment, the density matrix is expanded as a linear combination of a basis set of operators. The product operators resolve the density matrix into a set of elements that can be visualized as generalized magnetization vectors, often referred to as coherences. The motion of the product operators subjected to RF pulses, chemical shifts, and coupling is analogous to the motion of the classical magnetization vectors in three-dimensional space and thus the popular vector model can be extended to spin systems that contain scalar coupling.

Every interaction in NMR spectroscopy of liquids, e.g. chemical shift, scalar coupling, and RF pulses, can be formally represented as a rotation or sequence of rotations of a vector. All *orthogonal* rotations of any vector involve a maximum of three coordinates: the axis about which the vector is rotated and two axes that are orthogonal (90°) to the rotation axis. In NMR the dimension of the *state vector* which describes the spin system can be quite large. In coupled spin systems, a 16 dimensional vector is needed to describe the motion of two spins and a 64

dimensional vector is required for three coupled spins. In general, the dimensions of the space required to describe the spin motion in a system with N coupled spins is 4^N. However, all rotations occur in three dimensional *subspaces* involving only one rotation axis and two orthogonal axes. Many of these subspaces have no physical analog, but since they are three dimensional rotations, a picture of the rotations can be constructed by using a three dimensional framework with the appropriate labels for the axes. This all may seem very esoteric at this point, but as we proceed, rotations of multidimensional vectors will become quite descriptive.

In the previous paper in this series, the vector model was applied to isolated spin systems and related to the product operator formalism. In this paper the vector model will be extended in the framework of product operators to describe the motion of coupled spin systems.

Description of Coupling

For an ensemble of non-interacting spins in a magnetic field, the classical description of the magnetization as a vector gives results identical to the quantum mechanical description given by the density matrix treatment. It is only in the presence of scalar coupling or other strictly quantum mechanical interactions that the evolution of a spin system can not be described by classical mechanics. However, since most of the interesting and useful cases in modern NMR spectroscopy involve quantum mechanical interactions, the vector model must be abandoned or modified.

An intermediate approach to the description of NMR experiments involving scalar coupling is to use a classical vector model supplemented with results from quantum mechanics (See Benn and

Gunther (1983) and Turner(1984)). This approach, while lending some insight to the mechanics of some simple pulse sequences, can lead to misunderstandings and wrong conclusions about the behavior of the spin system. This approach completely fails to describe multiple quantum coherence. The density matrix treatment is the most complete description of the spin system that is possible. The product operator formalism is a shorthand form of the density matrix description that keeps the correctness of the density matrix treatment, but at the same time, allows the experimentalist to retain a semblance of intuition.

Coupled Spin Systems

From the viewpoint of the ^{13}C nucleus in a coupled spin system **I-S**, such as in a ^{13}C-^{1}H moiety, the system can be described as a mixture of two different compounds, one compound with the carbon attached to a ^{1}H spin up (α) and an almost equimolar amount of molecules with the carbon attached to a ^{1}H spin down (β). This description is commonly used to calculate the patterns of lines in a coupled spin system. For ^{13}C - ^{1}H the two species present are ^{13}C with a ^{1}H spin up and one with a spin down.

$^{13}C\ ^{1}H^{\alpha}$

$^{13}C\ ^{1}H^{\beta}$

Since there are nearly equal numbers of α and β H spins, there are two ^{13}C spectral lines of (nearly) equal intensity. The frequency difference between the peaks is due to the local magnetic field of the coupled ^{1}H spin, the α spin increases and the β spin decreases the magnetic field felt at the ^{13}C nucleus.

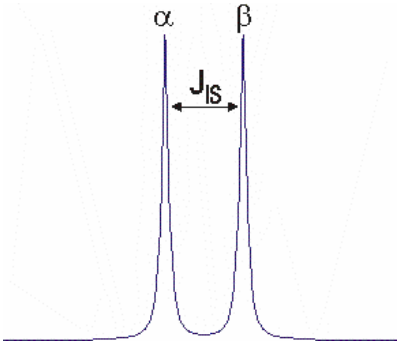

Figure 1. Doublet formed from the coupling of one spin with another spin ½ nucleus. The α and β labels refer to the spin states of the coupled nucleus that give rise to different local magnetic fields and thus different frequencies for the coupled spin.

The spectrum consists of two lines separated by the coupling constant J_{IS} in Hertz (Figure 1).

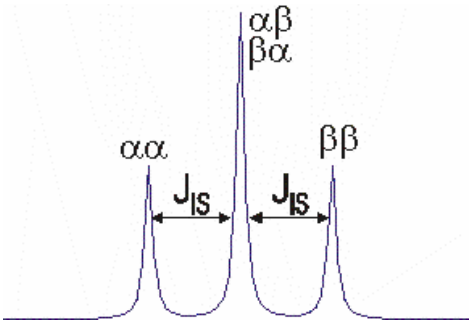

Figure 2. Triplet formed from the coupling of one spin with two other spin ½ nuclei. The coupling constants to the two coupled spins are identical. If the coupling constants were not identical then the αβ and βα states would differ in energy giving rise to 4 peaks.

For a C-H_2 moiety, We have one state with parallel ^{1}H spins up, two states with the ^{1}H spins aligned oppositely, one state with parallel ^{1}H spins down.

^{13}C - αα

^{13}C - αβ & βα

^{13}C - ββ

This gives a spectrum with three lines separated by J (assuming the same coupling constant for both ^{1}H spins) with an intensity ratio of 1:2:1 (Figure 2).

Similarly, for a methyl group CH_3 there are 4 possible states, which gives a spectrum containing 4 lines separated by J in a 1:3:3:1 intensity ratio (Figure 3).

^{13}C – ααα

^{13}C – ααβ αβα βαα

^{13}C – ββα βαβ αββ

^{13}C - βββ

The splitting of these lines in coupled systems arises from the nucleus being subjected to different magnetic fields depending on the arrangement of the coupled nuclei. This effect is a bit difficult to comprehend from the viewpoint of classical mechanics since the

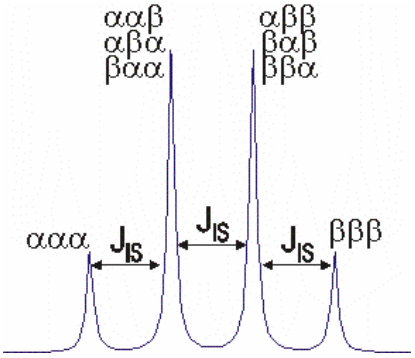

Figure 3. Quartet formed from the coupling of one spin with three other spin ½ nuclei. The coupling constants to the two coupled spins are identical.

interaction between two bar magnets (or two nuclear magnetic moments) averages to zero if every orientation is allowed. In solution, the molecule tumbles randomly and in a classical description the splitting should be averaged to zero. Quantum mechanics is strange; the splitting is invariant to molecular rotation.

2 Semiclassical Picture of Coupling

Before embarking on the product operator description of coupling, it is useful to obtain an intuitive picture of coupling through a semi-classical approach. This approach was described by Lynden-Bell et al.### Assume a heteronuclear spin system **I-S** with a non-zero scalar coupling between the two spins, $J_{IS} <> 0$, *e.g.* the coupled $^{1}H^{13}C$ in HC-Cl_3. A 90° pulse applied to $\mathbf{S_z}$ magnetization, generates transverse coherence $-\mathbf{S_y}$.

$$S_z \xrightarrow{\pi/2\widehat{S_x}} -S_y \tag{1}$$

The state vector $-\mathbf{S_y}$ is composed of vectors from two very nearly equal populations of

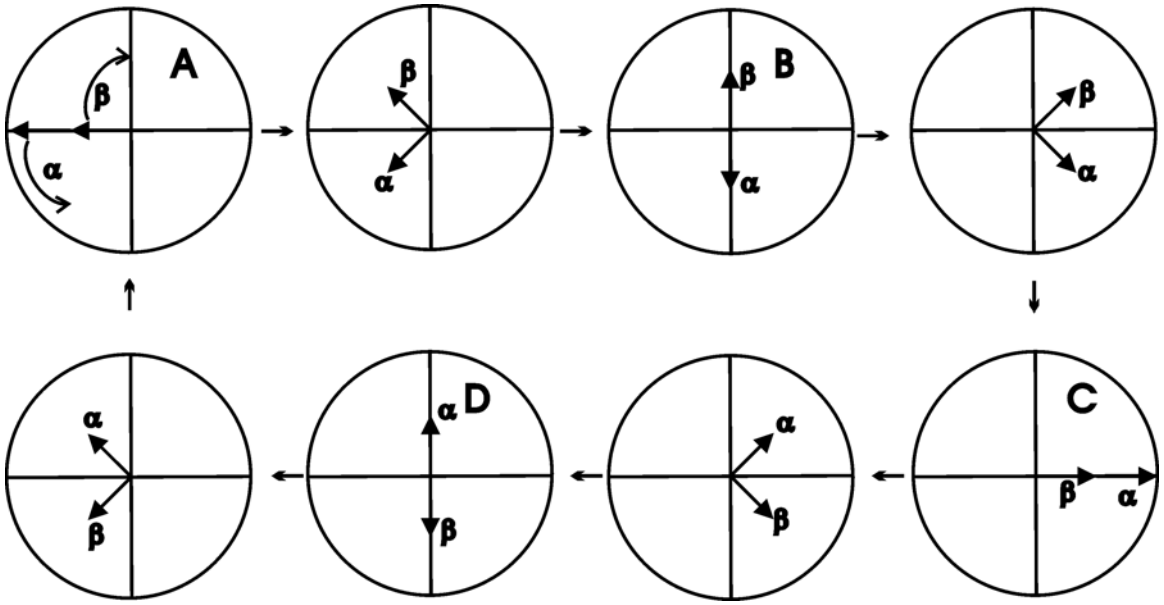

Figure 4. Evolution of a transverse spin **S** that is coupled to another spin **I** with states α and β.

molecules: those coupled to **I** spins in the α state and those coupled to **I** spins in the β state (Figure 4 position A). The local magnetic fields experienced by the **S** spins in these two populations are slightly different because of the different magnetic fields generated by the α and β **I** spins. Therefore, the two types of **S** spins have slightly different precession frequencies. For example, in a proton-coupled ^{13}C spectrum of chloroform, there are two resonance lines with the frequency difference being equal to the coupling constant. If the **S** spin is on resonance, *i.e.* the **S** frequency in the absence of coupling is zero in the rotating frame, then the two $-\mathbf{S_y}$ vectors arising from the that are attached to α and β **I** spins will precess apart from one another at the coupling frequency (Figure 4). At time $1/(2*J_{\mathbf{IS}})$, the two spin vectors will have precessed into opposite positions along the X coordinate axis (Figure 4 position B). As the spins continue to precess, the two vectors again become parallel along the Y axis at a total time of $1/J_{\mathbf{IS}}$ (Figure 4 position C). At a time of $3/2J_{\mathbf{IS}}$, the vectors will again be in opposite directions along the X axis. Note in (Figure 4 position D) that the α and β spins are negative with respect to the positions in (Figure 4 position B). Finally, at a time $2/J_{\mathbf{IS}}$ the spin vectors return to the -Y axis as in (Figure 4 position A).

The observed time domain signal is the sum of the two vectors that are precessing in the XY plane. When the vectors are aligned, a maximum signal will be observed. When the vectors are pointing in opposite directions, a zero signal will be observed. The observed signal due to the coupling can be represented as a cosine function, starting at a maximum, going through zero and a negative maximum, then returning through zero to the positive maximum. In this semi-classical picture, the observed magnetization vector changes magnitude, but it is not clear from this description as to where the magnetization goes when the observed signal is equal to zero.

Quantum Description - Anti-phase Coherence

For the evolution of an isolated spin vector evolving under chemical shift, we have Eqn 2.

$$-S_y \xrightarrow{\omega_s t \hat{I}_z} -S_y \cos(\omega_s t) + S_x \sin(\omega_s t) \quad (2)$$

If we construct an analogous relationship for the evolution under the coupling operator J_{IS} we obtain Eqn. 3.

$$-S_y \xrightarrow{J_{IS} t} -S_y \cos(J_{IS} t) + Q \sin(J_{IS} t) \quad (3)$$

Equation 3 represents the evolution of the $\mathbf{S_y}$ coherence as the precession of a single vector, which does not change in magnitude, about an axis $\mathbf{J_{IS}}$ in a plane spanned by two other coordinate axes $\mathbf{S_y}$ and **Q**. This is a three-dimensional space, but what are the axes **Q** and **J**? A schematic of this concept is shown in Figure 5.

Again referring to a semi-classical picture of a coupled spin system, the two counter-rotating components that arise from the S spin being attached to an α or β spin will evolve from along the Y axis (Figure 4 position A) to opposite directions along the X axis (Figure 4B) in the time $1/2*J_{IS}$, which rotates each component by 90^o around the Z axis. This evolution can be represented as Eqn. 4. The amount of each of the components is given by the

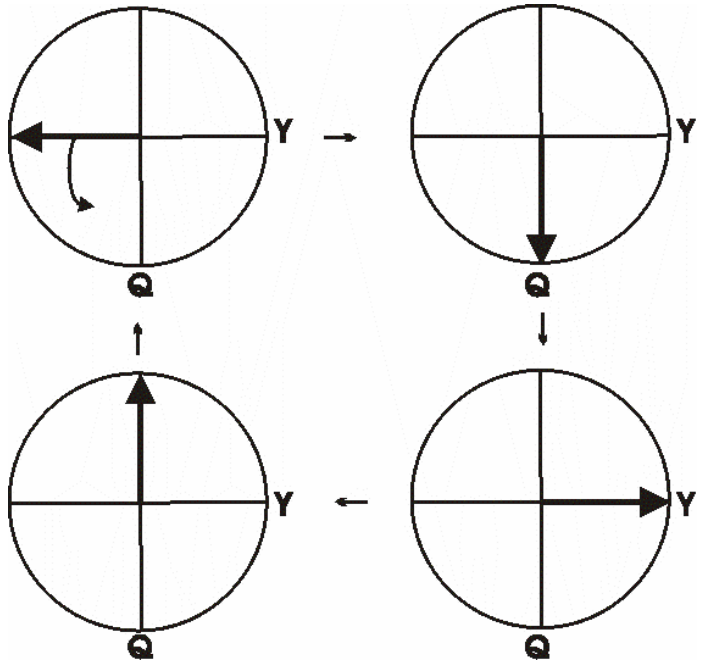

Figure 5. Rotation of a vector around a coupling axis (out of the plane) resulting in an oscillation between the Y axis and another axis Q.

population of the attached up and down

$$-\alpha S_y - \beta S_y \xrightarrow{(1/2)J_{IS}} \alpha S_x - \beta S_x \tag{4}$$

I spins, α and β respectively. The expression in Eqn. 4 can be rearranged to the form in Eqn. 5.

$$\alpha S_x - \beta S_x = (\alpha - \beta) S_x \tag{5}$$

The quantity (α-β) in Eqn. 5 represents the population difference across the **I** energy levels and, therefore, is equivalent to the longitudinal magnetization of the coupled spin $\mathbf{I_z}$. One must be careful here since we are so close to the edge between classical and quantum effects. More precisely, α-β is proportional to the expectation value $\mathbf{I_z}$. By substituting $\mathbf{I_z}$ for (α-β) one obtains Eqn 6.

$$(\alpha - \beta) S_x = I_z S_x \tag{6}$$

The evolution of Eqn. 4 can be rewritten as Eqn 7.

$$-S_y \xrightarrow{J_{IS}t} -S_y \cos(J_{IS}t) + 2I_z S_x \sin(J_{IS}t) \tag{7}$$

A normalizing factor of 2 has been included the $\mathbf{I_zS_x}$ term, but for the sake of simplicity the normalization factors will not be included in the remainder of the manuscript. The $\mathbf{I_zS_x}$ state in Eqn. 7 is known as $\mathbf{S_x}$ magnetization that is anti-phase with respect to **I**. This state is not directly observable under any experimental conditions, which is consistent with a picture involving the sum of oppositely pointed vectors. A more general term, *coherence*, is commonly used in place of magnetization for the description of non-observable terms. The term coherence is also often used to describe observable magnetization.

As described above, after arriving at the antiphase state in Eqn. 7, the **S** vector will continue to rotate and align along the $\mathbf{S_y}$ axis, and further rotate to the negative antiphase state $-\mathbf{I_zS_x}$, before

completing a full cycle back to $-\mathbf{S_y}$.

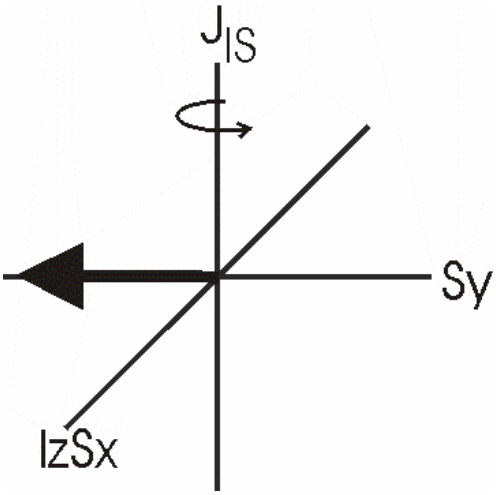

Figure 6. Right-handed coordinate system for **Sy** evolving under coupling $\mathbf{J_{IS}}$.

To represent the evolution of in-phase to anti-phase coherence in a vector picture, we must invent a new coordinate system that is consistent with the process in Eqn. 7. This can be simply done by generating a 3-dimensional coordinate system and labeling the transverse axes with $\mathbf{S_y}$, $\mathbf{I_zS_x}$ in a right-handed coordinate system ($\mathbf{I_zS_x}$ along the usual X axis and $\mathbf{S_y}$ along the usual Y axis).(Figure 6). The only remaining axis that is not known is that of the $\mathbf{J_{IS}}$ coupling operator. This can be easily obtained by following standard angular momentum commutation rules (Appendix ##), but as a visual aid it is useful to examine an algorithmic procedure to determine the rotation axis. We already have two of three axes in the three dimensional coordinate system and by invoking the rule that rotations of the **I** spin do not affect the **S** spin and *vice versa* (commutation of different spins) we can easily obtain the third axis. If there were a vector along the $\mathbf{I_zS_x}$ axis and a $-\pi/2$ rotation is applied around the $\mathbf{S_y}$ rotation, the **S** part of $\mathbf{I_zS_x}$ would be rotated to $\mathbf{S_z}$ **(**Fig. 7). The **I** part would be unaffected and the third axis would be $\mathbf{I_zS_z}$. This coordinate system can be used in the case of a coupled spin system just as the normal X, Y, Z system used for an isolated spin. Also just as in the

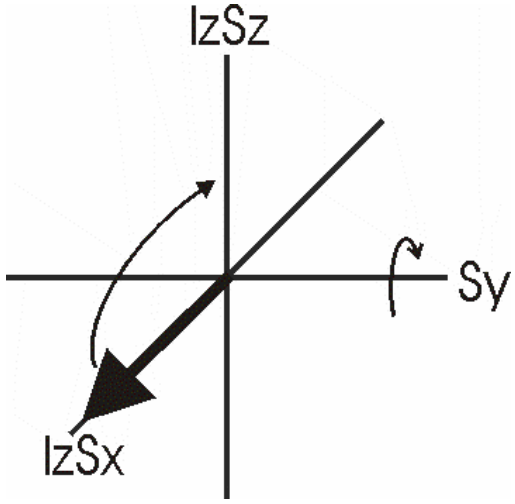

Figure 7. Generation of the proper third axis in a **IzSx-Sy** coordinate system by a $\pi/2$ rotation of a vector lying along **IzSx** around **Sy**.

isolated spin case, any one of these axes can be used as the rotation axis.

From this 3D coordinate system, the $\mathbf{J_{IS}}$ coupling rotation axis is $\mathbf{I_zS_z}$ and the **S** vector rotates between the $\mathbf{S_y}$ and $\mathbf{I_zS_x}$ axis in a counterclockwise direction for a positive rotation. While the axes are not labeled with familiar coordinates of an X,Y,Z system, the rules for calculation of the rotation are identical.

The time dependence can be written as in Eqn. 8.

$$-S_y \xrightarrow{\pi Jt\widehat{I_zS_z}} -S_y\cos(\pi Jt) + I_zS_x\sin(\pi Jt) \qquad (8)$$

Here the normalizing factor has been left out. The transverse magnetization oscillates between in-phase ($\mathbf{-S_y}$) and anti-phase coherence ($\mathbf{I_zS_x}$). (see Appendix A for further discussion of the generation of two spin product operator coordinate systems).

The $\mathbf{I_zS_z}$ operator arises from the form of the scalar coupling interaction J(**I•S)**, in the Hamiltonian. The dot product of **I** and **S** is $\mathbf{I_zS_z} + \mathbf{I_xS_x} + \mathbf{I_yS_y}$. In the weak coupling regime, where the difference in chemical shift between the two coupled spins is much greater than the coupling constant, terms arising from the rotation around $\mathbf{I_xS_x}$ and $\mathbf{I_yS_y}$ are oscillatory and average to zero over time. This leaves only $\mathbf{I_zS_z}$ for the weak coupling case. In the case of strong coupling, where the chemical shift difference and the coupling constants are similar, the transverse terms must be retained. The product operator formalism has been presented for the strong coupling case (##Kay ; Van de Ven). We will assume the weak coupling condition in all cases except where noted. This simplification is not a failing of this formalism, but the inclusion of strong coupling introduces unnecessary complications in the analysis of pulse sequences, unless one is specifically interested in the strong coupling regime.

Two-Spin Space

Without introduction of scalar coupling or other interactions, a space of three dimensions is sufficient to describe the behavior of nuclear spins. Even if two different types of non-interacting spins are under study, each spin inhabits its own universe (space) described by a unique three dimensional coordinate system (See Figure 8). It seems natural to think of each separate spin space as a whole, ignoring the other one. We can represent the state of the two spaces by the by two, three-dimensional vectors or by a single six-dimensional vector ($\mathbf{I_x}$, $\mathbf{I_y}$, $\mathbf{I_z}$, $\mathbf{S_x}$, $\mathbf{S_y}$, $\mathbf{S_z}$). Although it seems natural to think of these as separate spaces, it is just as easy to consider the total system as a single six-dimensional space. The components of the vectors are obtained by projecting them onto the six, mutually-orthogonal, axes of this space. It is not easy to grasp more than three dimensions in the minds-eye, but one can always envision three-dimensional sub-spaces of a higher dimensional space composed of three orthogonal axes of the three-dimensional subspace.

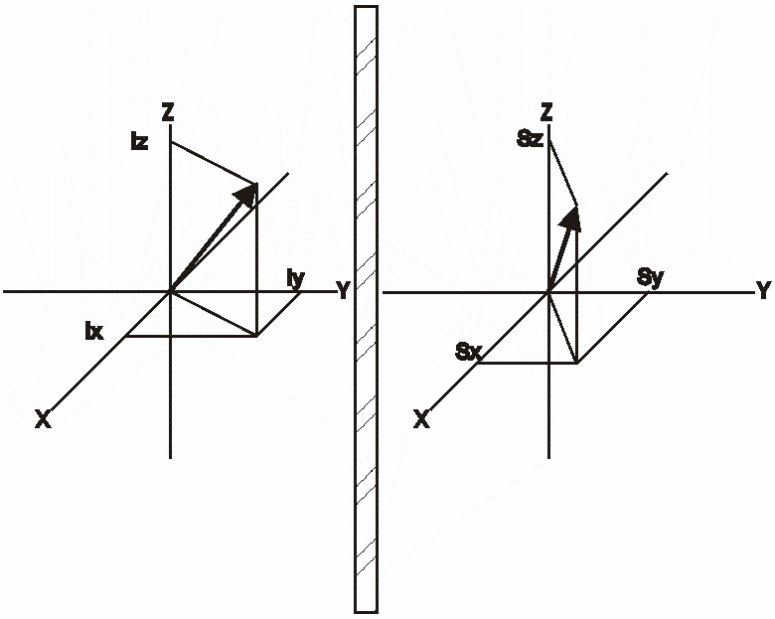

Figure 8. Representation of two isolated spins **I** and **S**. There is no interaction between the spins.

The introduction of coupling into a two spin system is analogous to poking a hole in the wall that separates the two universes shown in Figure 8 thus allowing the spins to feel the motion of the

other spin (Figure 9). To generate a space that contains two interacting spins, **I** and **S**, the **Ix**, **Iy**, **Iz**, **Sx**, **Sy**, and **Sz** operators must be represented along with the coupling interaction between the spins. However, we don't have any axes to spare, since all of the axes are in use describing the **x**, **y**, and **z** components of the two individual spins. To extend the classical vector analogy to include the coupling interaction, there must be at least one more axis that is orthogonal to both sets of three-dimensional Cartesian coordinates.

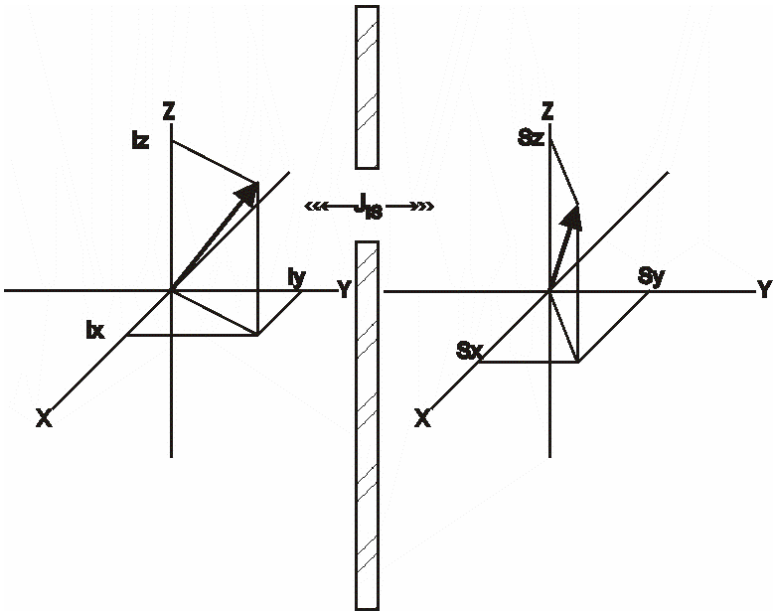

Figure 9. Representation of two coupled spins **I** and **S**. The hole in the barrier represents the coupling interaction between the spins. Now one spin can feel the effects of the other spin.

Two-Spin Product Operators

The terms that involve two operators (e.g. $\mathbf{I_zS_x}$) are similar to $\mathbf{S_x}$, $\mathbf{S_y}$, and $\mathbf{S_z}$ but describe coordinate axes that are in a space with more than three dimensions. In order to describe a spin system the space of the description must be large enough to hold all of the information necessary to completely define the system. For a single non-interacting spin the space consists of operators that correspond to the three spatial coordinate axes and an identity operator to complete the mathematical group. A spin **I** would have operators $\mathbf{I_x}$, $\mathbf{I_y}$, $\mathbf{I_z}$, and $\mathbf{I_E}$. The three operators $\mathbf{I_x}$, $\mathbf{I_y}$, and $\mathbf{I_z}$ are just the Cartesian coordinates for the classical magnetization vector for spin **I**. The $\mathbf{I_E}$

operator can be thought of as the bulk of magnetic spins that have equal populations (saturated state) in the α and β quantum mechanical energy levels and thus do not give rise to any net magnetization.

Table 1. Product operators and coherence orders for a coupled two-spin system.

Name	Coherence order	Operators	Observable?
Identity	0	$\mathbf{E}$	No
longitudinal	0	$\mathbf{I_z}$, $\mathbf{S_z}$	Yes (ODMR, magnetometer)
longitudinal two spin order	0	$\mathbf{I_zS_z}$	No
single quantum	±1	$\mathbf{I_x}$,$\mathbf{I_y}$,$\mathbf{S_x}$,$\mathbf{S_y}$	Yes
anti-phase single quantum	±1	$\mathbf{I_xS_z}$, $\mathbf{I_yS_z}$, $\mathbf{I_zS_x}$, $\mathbf{I_zS_y}$	Not directly- must evolve into single quantum terms under coupling
zero+double quantum	0, ±2	$\mathbf{I_xS_x}$, $\mathbf{I_xS_y}$, $\mathbf{I_yS_x}$, $\mathbf{I_yS_y}$	No

NOTE: A normalization constant equal to $2^{(\text{number of operators} - 1)}$ should multiply all of the product operators.

The coordinates (axes) that are required to describe a coupled two spin system are generated by the Kronecker products of the **I** and **S** spin operators. In the product operator formalism, the Kronecker products can be obtained by taking all possible of the combinations of the **I** and **S** operators ($\mathbf{I_E}$, $\mathbf{I_x}$, $\mathbf{I_y}$, $\mathbf{I_z}$, $\mathbf{S_e}$, $\mathbf{S_x}$, $\mathbf{S_y}$, $\mathbf{S_z}$). The resultant 16 operators along with their coherence orders are listed in Table 1. Mathematically, the order of the operators is important in generating the Kronecker products, however there exists a permutation matrix that transforms $\mathbf{I}\otimes\mathbf{S}$ to $\mathbf{S}\otimes\mathbf{I}$. We will consider $\mathbf{I_xS_z}$ as being identical to $\mathbf{S_zI_x}$. Extension of the product operators to more than two coupled spins is made by taking all combinations of the **E**, **X**, **Y**, and **Z** operators for each coupled spin. As an example in a system with 4 spins, operators of the type $\mathbf{I_xS_zT_yP_z}$ can be obtained. There are 256 (4^N) different operators in this spin space.

The *only* physically observable operators are the terms $\mathbf{I_x}$, $\mathbf{I_y}$, $\mathbf{S_x}$, and $\mathbf{S_y}$ with coherence order 1 corresponding to transverse magnetization that induces current in the receiver coil. The coherence order of operators can easily be determined by expressing them as raising and lowering operators and summing the pluses and minuses (Eqn. 9).

$$\begin{aligned} I^+ &= I_x + iI_y \\ I^- &= I_x - iI_y \\ I_x &= 1/2(I^+ + I^-) \\ I_y &= -i/2(I^+ - I^-) \end{aligned} \tag{9}$$

$\mathbf{I_z}$ and $\mathbf{S_z}$, which have coherence order 0, are physically observable terms but are not measured directly by NMR techniques. The anti-phase single quantum terms, *e.g.* $\mathbf{I_zS_x}$, which can be written as $\mathbf{I_zS^+ + I_zS^-}$, have coherence order 1 but are formally not directly observable. These terms can evolve into observable terms during a free precession period during which the scalar coupling operator is active (Eqn. 10).

$$I_z S_x \xrightarrow{\pi J t \widehat{I_z S_z}} I_z S_x \cos(\pi J t) + S_y \sin(\pi J t) \tag{10}$$

In the majority of experiments the anti-phase coherences are the important terms in understanding how the experiment works. The vector picture of this evolution is not the same as in Figure 7, since the coordinates in Eqn. 10 are $\mathbf{S_x}$, $\mathbf{I_zS_y}$, and $\mathbf{I_zS_z}$. The proper coordinate system is given in Figure 10. See Appendix A for an algorithmic approach for generating product operator coordinate systems.

The terms with two transverse operators are mixtures of 0 and ±2 coherence (for example see Eqn 11.) and are not observable. The longitudinal two spin order term $\mathbf{I_zS_z}$ has coherence order 0 and is also not observable. The non-observable terms can be turned into observable terms by combinations of RF pulses and evolution under the coupling operator.

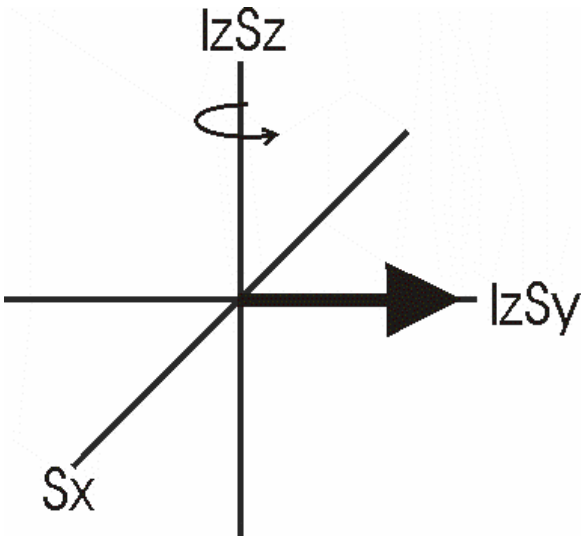

Figure 10. Three dimensional coordinate system for the evolution of $\mathbf{S_x}$ under the $\mathbf{I_zS_z}$ coupling operator**.**

$$I_x S_x \propto \left(I^+ + I^-\right) * \left(S^+ + S^-\right) = I^+S^+ + I^+S^- + I^-S^+ + I^-S^- \tag{11}$$

The product operators in Table 1 can be used in the absence of relaxation to completely describe the evolution of a coupled two-spin system during an arbitrary pulse sequence. The 16 product operators that are generated by this procedure can be viewed as the spherically-symmetric identity operator **E** and 15 coordinate axes that are necessary to describe an arbitrary state vector of the two interacting spins. Having more than three dimensions may seem difficult to visualize, but it is no more difficult than having a series of experiments with coordinates of *e.g.* [pH, temperature, ionic strength, concentration, E. coli strain] that span a 5 dimensional vector space. The extension of the product operator formalism to larger spin systems is straightforward.

In the first paper of this series(##), the spin echo sequence performed on an isolated spin was described. That analysis is repeated here, with a slight modification, in order to contrast and

compare the behavior of an isolated spin with that of a coupled spin system.

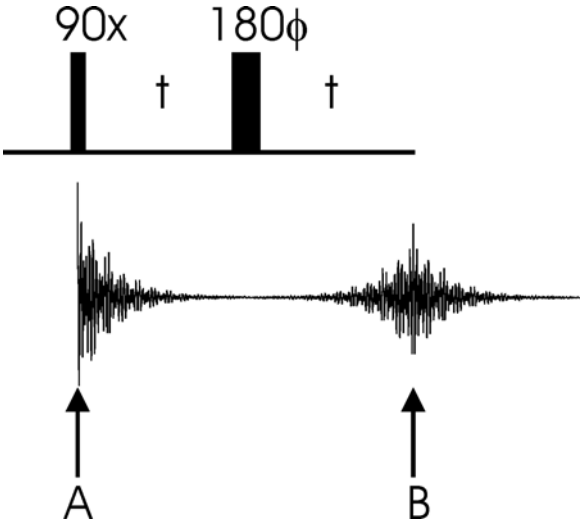

Figure 11. Pulse sequence and time domain signal for a spin echo experiment.

Spin echo: Isolated spin system

A spin echo sequence, which is a pulse-interrupted free precession period with a π pulse placed at the midpoint (τ - 180_{ϕ} - τ), refocuses the chemical shift (and any dephasing due to field inhomogeneity) of a transverse isolated spin, creating an effective Hamiltonian operator that does not contain a chemical shift operator. This sequence does not alter the state of the spin system except for a possible phase shift.

Figure 11 is the pulse sequence for a spin echo sequence applied to a single isolated spin **I**. An initial 90° pulse rotates the spin from the Z axis into the transverse plane. Beneath the pulse sequence in Figure 11 is the time domain signal that would be observed if the receiver was turned on after the initial 90° pulse. The complicated oscillations in the signal are due to the interference between vectors precessing at different frequencies. The signal decays away due to both relaxation and inhomogeneities in the magnetic field. The spin echo cannot refocus the effects of relaxation but only the decay due to dephasing caused by inhomogeneities in the magnetic field. This is shown as decreased amplitude of the echo at point B compared to that of the original amplitude A. In this sequence the receiver is usually turned on at point B.

$$
\begin{aligned}
I_z \quad &\xrightarrow{\pi/2\hat{I}_x} \quad -I_y \\
&\xrightarrow{\omega t_1 \hat{I}_z} \quad -I_y\cos(\omega t_1) + I_x \sin(\omega t_1) \\
&\xrightarrow{\pi \hat{I}_x} \quad I_y \cos(\omega t_1) + I_x \sin(\omega t_1) \\
&\xrightarrow{\omega t_2 \hat{I}_z} \quad \left[I_y \cos(\omega t_2) - I_x \sin(\omega t_2) \right] \cos(\omega t_1) \\
&\qquad\qquad + \left[I_x \cos(\omega t_2) + I_y \sin(\omega t_2) \right] \sin(\omega t_1)
\end{aligned}
\tag{12}
$$

if $t_1 = t_2 = t$

$$
\begin{aligned}
&= I_y[\cos^2(\omega t) + \sin^2(\omega t)] \\
&= I_y
\end{aligned}
$$

The product operator description for this sequence is in Eqns. 12. At the end of the sequence, there is no contribution due to the frequency (chemical shift) of the signal. All signals would behave the same behavior irrespective of the frequency. This result could be obtained formally by a single rotation of $\mathbf{I_z}$ by a -90˚ pulse around the X axis (Eqn. 13).

$$
I_z \xrightarrow{-\pi/2\hat{I}_x} I_y \tag{13}
$$

Beyond point B (Figure 11), the vectors again precess around the Z axis and dephase due to chemical shift and field inhomogeneities. During this time the receiver would usually be turned on. The resultant signal would be digitized and stored. A Fourier transform of the signal would give the normal NMR spectrum of the system.

A series of **i** rotations $\hat{U}_i$ representing the various Hamiltonian operators during the pulse sequence can be written as in Equation 14.

$$\sigma_0 \xrightarrow{\left(\theta\hat{U}\right)_1} \xrightarrow{\left(\theta\hat{U}\right)_2} \xrightarrow{\left(\theta\hat{U}\right)_3} \xrightarrow{\left(\theta\hat{U}\right)_4} \cdots \xrightarrow{\left(\theta\hat{U}\right)_i} \sigma_t \qquad (14)$$

These distinct rotations can always be combined into a single total rotation applied to σ_0 (Eqn. 15).

$$\sigma_0 \xrightarrow{\left(\theta\hat{U}\right)_{total}} \sigma_t \qquad (15)$$

In many cases, $\left(\theta\hat{U}\right)_{total}$ is a single rotation or at most a short series of a few rotations. By reducing the pulse sequence to a series of simple propagators, the experimental pulse sequence can be calculated and described in a simple and straightforward manner.

The sequence of the rotation operators for the spin echo sequence for an isolated spin is given in Equation 16.

$$\xrightarrow{\pi/2\hat{I}} \xrightarrow{\omega t\hat{I}_z} \xrightarrow{\pi\hat{I}_\phi} \xrightarrow{\omega t\hat{I}_z} \qquad (16)$$

With the process described in the previous paper(##), this sequence can be simplified to the two rotations shown in Eqn 17.

$$\xrightarrow{\pi/2\hat{I}_x} \xrightarrow{\pi\hat{I}_\phi} \qquad (17)$$

The final phase of the spin depends only on the phase of the 180° pulse, no chemical shift evolution (rotation about the Z axis) occurs. This is also equivalent to the refocusing of spin isochromats in an inhomogeneous magnetic field, where the chemical shift operator is replaced by a spatially-varying (inhomogeneous) magnetic field.

Coupled Two-Spin System – No pulses

It is useful to investigate the behavior of a coupled spin system during free precession and then contrast that behavior with sequences that have π pulses inserted midway through the free precession period. Figure 12 shows the pulse sequence and the vector picture of the spins. After rotation of $\mathbf{I_z}$ magnetization into the transverse plane, the **I** spin rotates due to both

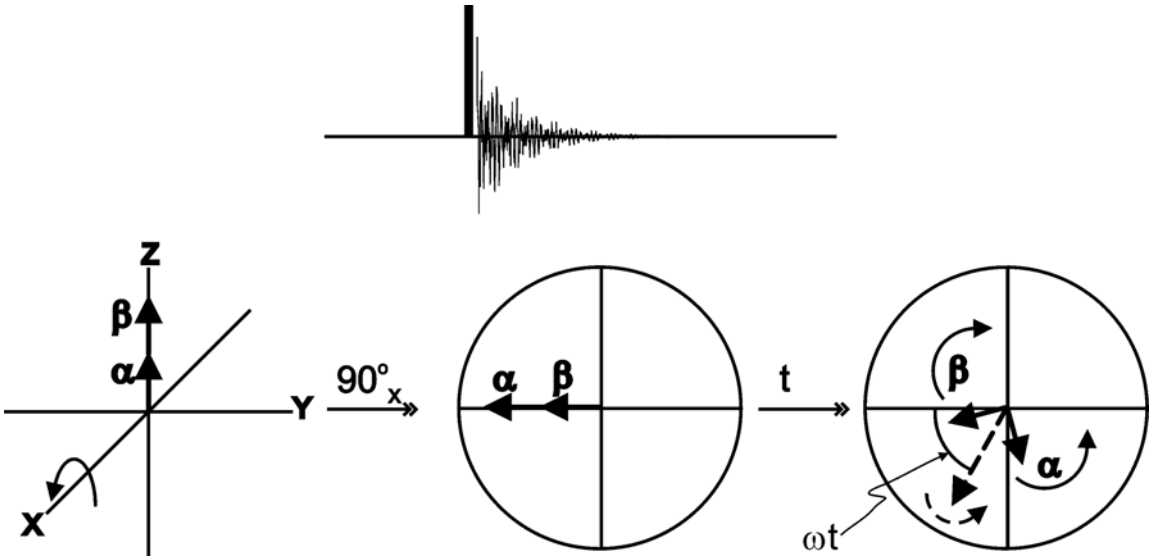

Figure 12. Pulse sequence and vector picture of the evolution of a **IS** coupled spin system. The dashed vector at an angle of ωt in the rightmost panel represents the chemical shift of the spin system in the absence of coupling. The vectors labeled α and β are the two components of the doublet.

chemical shift (rotation around the Z axis) and scalar coupling to the **S** spin that causes counter rotating **I** vectors corresponding to **I** spins coupled to α and β **S** spins. Since no other interactions are applied during the sequence, the spins continue under this Hamiltonian for the entire period. Eqn. 18 shows the operators that act during this pulse sequence. There is no easy simplification of this sequence.

$$\xrightarrow{\pi/2\widehat{I_x}} \xrightarrow{\pi J_{IS} t \widehat{I_z S_z}} \xrightarrow{\omega_I t \widehat{I_z}} \xrightarrow{\omega_S t \widehat{S_z}} \qquad (18)$$

In the next section Eqn. 19has the full product operator description for this sequence, where t_1 is equal to the full period of evolution. The $\omega_S t\widehat{S_z}$ operator does not impact this sequence since the **S** spin remains along the Z axis for the entire period.

Coupled Two-Spin System - Selective I 180˚ pulse

Now we will analyze several variants of the a coupled, two-spin system subjected to a period of free precession interrupted with π pulses on the **I** and or **S** spins . The first sequence, which is identical to the spin echo sequence described above, consists of a π pulse on the excited, transverse spin, **I**, placed at the center of the evolution period with no pulse on the coupled partner **S**. Figure 13 shows the pulse sequence and vector picture for this sequence. For simplicity in the figure, the frequency of **I** in the absence of coupling is set to zero. This means that the vector would not precess around the Z axis in the absence of coupling. Even in the presence of a nonzero chemical shift, the results remain the same as will be shown by product operators. The **I** spins are divided into two separate vectors representing the **I** spins coupled to an **S** spin in the α state and the **I** spins coupled to an **S** spin in the β state. As discussed above, the presence of an α or β **S** spin will alter the magnetic field that

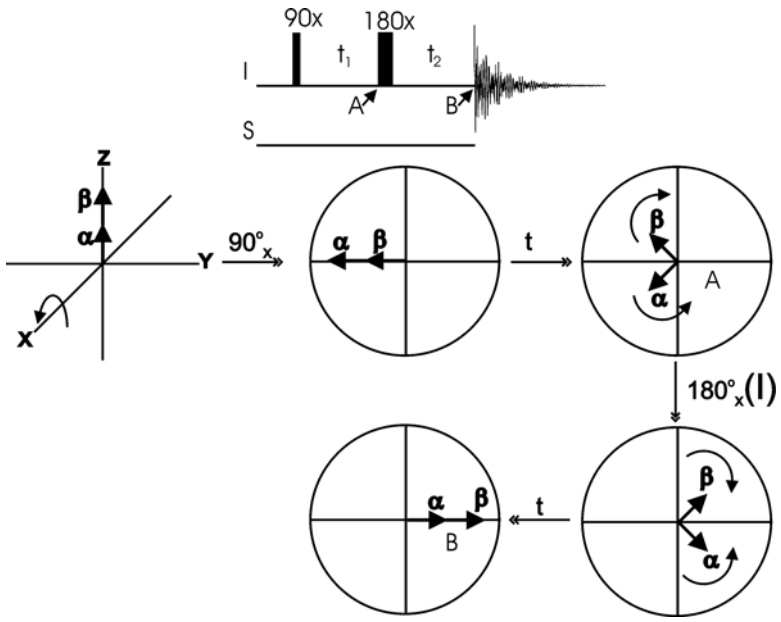

Figure 13. Pulse sequence and vector picture for a spin echo sequence applied to a **IS** coupled spin system. Here a selective π $\mathbf{I_x}$ pulse is applied midway in the evolution period 2t.

the **I** spins experiences and therefore the two vectors will have different frequencies. The vectors precess around the coupling axis during the first delay. The π pulse along the X axis applied only to the **I** spin mirrors the vectors across the X axis. During the final delay the vectors refocus along the Y axis. This is the identical behavior seen in an isolated **I** spin system (See Eqn. 17). This pulse sequence eliminates the interaction between the **I** and **S** spins, in other words they are decoupled.

The product operator description for Figure 13 is presented below (Eqns. 19). In this description, spin **I** is assumed to have a non-zero chemical shift. For completeness, all rotations are retained for the entire pulse sequence.

$$
\begin{aligned}
I_z + S_z \xrightarrow{\pi/2\widehat{I_x}} \quad & -I_y + S_z \\
\xrightarrow{\omega_I t\widehat{I}} \quad & -I_y\cos(\omega_I t_1) + I_x\sin(\omega_I t_1) + S_z \\
\xrightarrow{\omega_S t\widehat{S_z}} \quad & -I_y\cos(\omega_I t_1) + I_x\sin(\omega_I t_1) + S_z \\
\xrightarrow{\pi J_{IS} t_1 \widehat{I_z S_z}} \quad & \left[-I_y\cos(\pi J_{IS} t_1) + I_x S_z \sin(\pi J_{IS} t_1)\right]\cos(\omega_I t_1) \\
& +\left[I_x\cos(\pi J_{IS} t_1) + I_y S_z \sin(\pi J_{IS} t_1)\right]\sin(\omega_I t_1) + S_z
\end{aligned}
\qquad (19)
$$

Equation 19 is the product operator calculation to point A in Figure 13. The order of computation of the evolution under $\widehat{I_z}$, $\widehat{S_z}$, and $\widehat{I_z S_z}$ is arbitrary since all of these rotation operators commute with one another. Note also that since the **S** spin is never pulsed, the initial $\mathbf{S_z}$ could have been dropped from the analysis. Furthermore, since $\mathbf{S_x}$ or $\mathbf{S_y}$, is never generated, the chemical shift operator $\hat{\mathbf{S}}_\mathbf{z}$ does not have any effect and could also be eliminated. This will not be the case if the initial state of the **S** spin is not $\mathbf{S_z}$ In Eqn. 20 the analysis is picked up at the $\pi\mathbf{I_x}$ pulse and continues to point B of Figure 13.

$$
\begin{aligned}
\xrightarrow{\pi \widehat{I_x}} \quad & \left[I_y \cos(\pi J_{IS} t_1) + I_x S_z \sin(\pi J_{IS} t_1) \right] \cos(\omega_I t_1) \\
& + \left[I_x \cos(\pi J_{IS} t_1) - I_y S_z \sin(\pi J_{IS} t_1) \right] \sin(\omega_I t_1) + S_z \\
\xrightarrow{\omega_I t_2 \widehat{I_z}} \quad & \left[I_y \cos(\omega_I t_2) - I_x \sin(\omega_I t_2) \right] \cos(\pi J_{IS} t_1) \cos(\omega_I t_1) \\
& + \left[I_x S_z \cos(\omega_I t_2) - I_y S_z \sin(\omega_I t_2) \right] \sin(\pi J_{IS} t_1) \cos(\omega_I t_1) \\
& + \left[I_x \cos(\omega_I t_2) + I_y \sin(\omega_I t_2) \right] \cos(\pi J_{IS} t_1) \sin(\omega_I t_1) \\
& + \left[-I_y S_z \cos(\omega_I t_2) + I_x S_z \sin(\omega_I t_2) \right] \sin(\pi J_{IS} t_1) \sin(\omega_I t_1) + S_z \\
\xrightarrow{\pi J_{IS} t_2 \widehat{I_z S_z}} \quad & \left[I_y \cos(\pi J_{IS} t_2) - I_x S_z \sin(\pi J_{IS} t_1) \right] \cos(\pi J_{IS} t_1) \cos(\omega_I t_1) \cos(\omega_I t_2) \\
& + \left[-I_x \cos(\pi J_{IS} t_2) + I_y S_z \sin(\pi J_{IS} t_2) \right] \cos(\pi J_{IS} t_1) \cos(\omega_I t_1) \sin(\omega_I t_2) \\
& + \left[I_x S_z \cos(\pi J_{IS} t_2) + I_y \sin(\pi J_{IS} t_2) \right] \sin(\pi J_{IS} t_1) \cos(\omega_I t_1) \cos(\omega_I t_2) \\
& + \left[-I_y S_z \cos(\pi J_{IS} t_2) + I_x \sin(\pi J_{IS} t_2) \right] \sin(\pi J_{IS} t_1) \cos(\omega_I t_1) \sin(\omega_I t_2) \\
& + \left[I_x \cos(\pi J_{IS} t_2) + I_y S_z \sin(\pi J_{IS} t_2) \right] \cos(\pi J_{IS} t_1) \sin(\omega_I t_1) \cos(\omega_I t_2) \\
& + \left[I_y \cos(\pi J_{IS} t_2) - I_x S_z \sin(\pi J_{IS} t_2) \right] \cos(\pi J_{IS} t_1) \sin(\omega_I t_1) \sin(\omega_I t_2) \\
& + \left[-I_y S_z \cos(\pi J_{IS} t_2) + I_x \sin(\pi J_{IS} t_2) \right] \sin(\pi J_{IS} t_1) \sin(\omega_I t_1) \cos(\omega_I t_2) \\
& + \left[I_x S_z \cos(\pi J_{IS} t_2) + I_y \sin(\pi J_{IS} t_2) \right] \sin(\pi J_{IS} t_1) \sin(\omega_I t_1) \sin(\omega_I t_2) \\
& + S_z
\end{aligned}
\tag{20}
$$

With t_1 equal to t_2, this collection of operators and trigonometric functions simplifies to Equation 21.

$$
I_y + S_z \tag{21}
$$

This simple result was obvious from the vector picture, but the product operator approach generated a large number of terms that eventually canceled. This pulse sequence is very short and simple; many pulse sequences contain tens of pulses and evolution delays. The number of trigonometric terms involved in the analysis quickly becomes overwhelming. By analogy to the isolated spin case, it would seem that there should be simplifications that can be made by manipulating the rotation operators.

The rotation operators for this sequence are given in Equation 22. Again note that for a weakly coupled spin system the order of the terms during the free precession delays is arbitrary. This is not the case, however, for the order of the pulses and delays. The order of terms in a free precession delay does matter if the spin system has strong coupling, in fact, the chemical shift and the coupling rotations cannot performed separately, but must be carried out simultaneously. This complicates the product operator approach without adding much to the overall understanding. The assumption of weak coupling will be used here.

$$\xrightarrow{\pi/2\hat{I}_x}\xrightarrow{\omega_S t_1 \hat{S}_z}\xrightarrow{\omega_I t_1 \hat{I}_z}\xrightarrow{\pi J_{IS} t_1 \widehat{I_z S_z}}\xrightarrow{\pi \hat{I}_x}\xrightarrow{\pi J_{IS} t_2 \widehat{I_z S_z}}\xrightarrow{\omega_I t_2 \hat{I}_z}\xrightarrow{\omega_S t_2 \hat{S}_z} \quad (22)$$

Following the method presented in paper 1 of this series (##), an identity operator can be introduced without changing the behavior of the pulse sequence (Eqn 23).

$$\xrightarrow{\pi/2\hat{I}_x}\xrightarrow{\omega_S t_1 \hat{S}_z}\xrightarrow{\omega_I t_1 \hat{I}_z}\left[\xrightarrow{\pi \hat{I}_x}\xrightarrow{-\pi \hat{I}_x}\right]\xrightarrow{\pi J_{IS} t_1 \widehat{I_z S_z}}\xrightarrow{\pi \hat{I}_x}\xrightarrow{\pi J_{IS} t_2 \widehat{I_z S_z}}\xrightarrow{\omega_I t_2 \hat{I}_z}\xrightarrow{\omega_S t_2 \hat{S}_z} \quad (23)$$

The bracketed rotations marked in Equation 24 can be simplified (Appendix B##).

$$\xrightarrow{\pi/2\hat{I}_x}\xrightarrow{\omega_S t_1 \hat{S}_z}\xrightarrow{\omega_I t_1 \hat{I}_z}\xrightarrow{\pi \hat{I}_x}\left[\xrightarrow{-\pi \hat{I}_x}\xrightarrow{\pi J_{IS} t_1 \widehat{I_z S_z}}\xrightarrow{\pi \hat{I}_x}\right]\xrightarrow{\pi J_{IS} t_2 \widehat{I_z S_z}}\xrightarrow{\omega_I t_2 \hat{I}_z}\xrightarrow{\omega_S t_2 \hat{S}_z} \quad (24)$$

The operators in the brackets simplify to the operator in Eqn. 25.

$$\xrightarrow{-\pi J_{IS} t_1 \widehat{I_z S_z}} \tag{25}$$

Substituting, Eqn. 26 is obtained.

$$\xrightarrow{\pi/2\widehat{I_x}} \xrightarrow{\omega_S t_1 \widehat{S_z}} \xrightarrow{\omega_I t_1 \widehat{I_z}} \xrightarrow{\pi \widehat{I_x}} \left[\xrightarrow{-\pi J_{IS} t_1 \widehat{I_z S_z}} \xrightarrow{\pi J_{IS} t_2 \widehat{I_z S_z}} \right] \xrightarrow{\omega_I t_2 \widehat{I_z}} \xrightarrow{\omega_S t_2 \widehat{S_z}} \tag{26}$$

When $\mathbf{t_1} = \mathbf{t_2} = \mathbf{t}$, the bracket terms in Eqn. 26 are counter-rotating operators and are equal to the identity operator. Simplifying by removing the identity rotation, Eqn. 27 is obtained.

$$\xrightarrow{\pi/2\widehat{I_x}} \xrightarrow{\omega_S t \widehat{S_z}} \xrightarrow{\omega_I t \widehat{I_z}} \xrightarrow{\pi \widehat{I_x}} \xrightarrow{\omega_I t \widehat{I_z}} \xrightarrow{\omega_S t \widehat{S_z}} \tag{27}$$

The coupling operator has been eliminated. Except for the $\omega_S t\widehat{S_z}$ operators, sequence is now the same as that for the isolated spin (Eqn 16) with a $\pi\mathbf{I_x}$ pulse. Since rotation operators of different spins commute, the ordering of the **S** and **I** operators is arbitrary and the $\omega_S t\widehat{S_z}$ operators can be combined as in Eqn. 28.

$$\xrightarrow{\pi/2\widehat{I_x}} \xrightarrow{\omega_I t \widehat{I_z}} \xrightarrow{\pi \widehat{I_x}} \xrightarrow{\omega_I t \widehat{I_z}} \xrightarrow{\omega_S (2t) \widehat{S_z}} \tag{28}$$

Now the first four rotations are the same as for the isolated spin and can be simplified to Eqn. 29.

$$\begin{aligned} &\xrightarrow{\pi/2\widehat{I_x}} \xrightarrow{\pi \widehat{I_x}} \xrightarrow{\omega_S (2t) \widehat{S_z}} \\ &\equiv \xrightarrow{3\pi/2\widehat{I_x}} \xrightarrow{\omega_S (2t) \widehat{S_z}} \end{aligned} \tag{29}$$

Now the computation goes as in Equation 30.

$$I_z + S_z \xrightarrow{3\pi/2\hat{I}_x} I_y + S_z \xrightarrow{\omega_S (2t)\hat{S}_z} I_y + S_z \tag{30}$$

The simplicity of the vector picture has now been translated into a rigorous mathematical

computation.

Coupled Two-Spin System - Selective S 180˚ pulse

A related sequence to that of Figure 13 is one where the 180˚ pulse is placed in the center of the delay but on the **S** spin. The similarity of this pulse sequence to that in Figure 14 makes an interesting comparison.

The vector picture for this sequence is shown in Figure 14. After the initial 90˚ the vectors of spin **I** coupled to α **S** spins and those coupled to β **S** spins can be treated separately. The local field arising from the α **S** spin causes the coupled **I** spin to precess counter-clockwise (positive) during the t_1 delay, while the **I** spin coupled to the β **S** spin precesses clockwise. Precession due to chemical shift would also affect the trajectory of the vectors, but for clarity the chemical shift of the **I** spin is set to zero. The action of the 180˚ pulse on the **S** spin is to swap the α and β spin states of **S**. This causes the labels on the **I** spin vectors to exchange. Now the **I** spin vector that originally was coupled to an α **S** spin is now coupled to a β spin and will now precess in a clockwise (negative) direction. Similarly, the other **I** spin vector changes the direction of precession since it is now coupled to the α **S** spin. At the

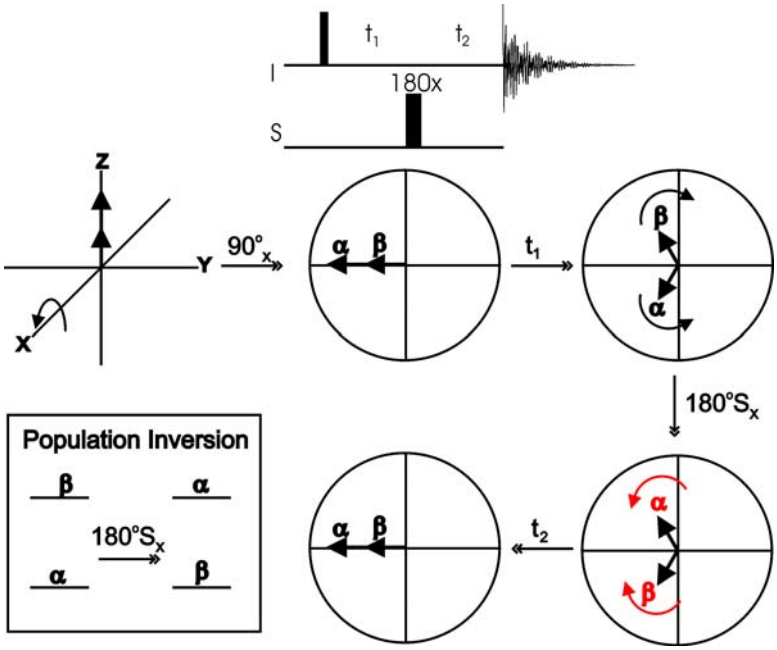

Figure 14. Pulse sequence and vector picture for evolution of an **IS** spin system where a π **S** pulse is introduced midway in the free precession of **I** spin evolution. Note that the π**S** pulse exchanges the αand β states of **S** (red)**.**

end of delay t_2, the **I** spins refocus with respect to the coupling. Had we included a nonzero chemical shift, however, the **I** spin vectors would have precessed at their characteristic chemical shift and would not be refocused with respect to chemical shift.

The sequence of rotations this sequence is given in Equation 31.

$$\xrightarrow{\pi/2\hat{I}_x}\xrightarrow{\omega_S t_1\hat{S}_z}\xrightarrow{\omega_I t_1\hat{I}_z}\xrightarrow{\pi J_{IS}t_1\hat{I}_z\hat{S}_z}\xrightarrow{\pi\hat{S}_x}\xrightarrow{\pi J_{IS}t_2\hat{I}_z\hat{S}_z}\xrightarrow{\omega_I t_2\hat{I}_z}\xrightarrow{\omega_S t_2\hat{S}_z} \tag{31}$$

The full product operator calculation would again involve the calculation of a large number of operators and trigonometric functions; however, by using the composite rotation methodology, a number of steps can be saved along with the avoidance of possible errors.

$$\xrightarrow{\pi/2\hat{I}_x}\xrightarrow{\omega_S t_1\hat{S}_z}\xrightarrow{\omega_I t_1\hat{I}_z}\xrightarrow{\pi J_{IS}t_1\hat{I}_z\hat{S}_z}\left[\xrightarrow{\pi\hat{S}_x}\xrightarrow{\pi J_{IS}t_2\hat{I}_z\hat{S}_z}\xrightarrow{-\pi\hat{S}_x}\right]\xrightarrow{\pi\hat{S}_x}\xrightarrow{\omega_I t_2\hat{I}_z}\xrightarrow{\omega_S t_2\hat{S}_z} \tag{32}$$

Introducing an identity rotation ($-\pi\hat{S}_x\ \pi\hat{S}_x$) into Eqn. 31 and then simplifying the bracketed terms marked in in Eqn 32., Eqn. 33 is obtained.

$$\xrightarrow{\pi/2\hat{I}_x}\xrightarrow{\omega_S t_1\hat{S}_z}\xrightarrow{\omega_I t_1\hat{I}_z}\xrightarrow{\pi J_{IS}t_1\hat{I}_z\hat{S}_z}\xrightarrow{-\pi J_{IS}t_2\hat{I}_z\hat{S}_z}\xrightarrow{\pi\hat{S}_x}\xrightarrow{\omega_I t_2\hat{I}_z}\xrightarrow{\omega_S t_2\hat{S}_z} \tag{33}$$

Removing the identity element of the two counter rotating $\hat{\mathbf{I}}_z\hat{\mathbf{S}}_z$ terms, Eqn. 34 is obtained.

$$\xrightarrow{\pi/2\widehat{I}_x} \xrightarrow{\omega_S t_1 \widehat{S}_z} \xrightarrow{\omega_I t_1 \widehat{I}_z} \xrightarrow{\pi \widehat{S}_x} \xrightarrow{\omega_I t_2 \widehat{I}_z} \xrightarrow{\omega_S t_2 \widehat{S}_z} \quad (34)$$

Since **S** rotations do not affect **I** spins and the **S** spins are never excited into the transverse plane in this experiment, the **S** terms can be removed leaving Eqn. 35, where **t'** is equal to $\mathbf{t_1+t_2}$. In the general case, where **S** there may be transverse **S** terms, the **S** rotations can not be removed.

$$\xrightarrow{\pi/2\widehat{I}_x} \xrightarrow{\omega_I t' \widehat{I}_z} \quad (35)$$

The overall effect of the 180° **S** pulse is to eliminate the coupling between the **I** and **S** spins (decoupling). If a 180° pulse applied in the center of a precession period to either spin of the coupled pair, the coupling interaction, on average, is eliminated at the end of the precession period. If the signal is sampled only at the end of the free precession period, then it will appear that the spin is not coupled. However, sampling at times when the 180° pulse is not in the center of the free precession period will let a portion of the coupling to remain since the coupling terms in Eqn. 33 will not be opposite and equal.

Coupled Two-Spin System - Simultaneous I and S 180° Pulses

The third example of the effects of 180° pulses during free precession periods is where both **I** and **S** 180° pulses are applied at

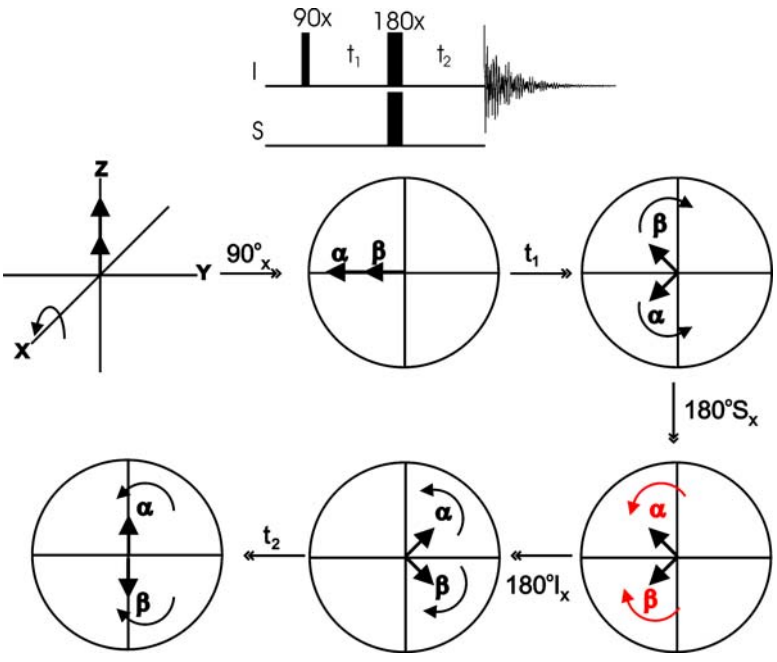

Figure 15. Pulse sequence and vector picture for a pulse interrupted free precession with simultaneous π**I** and π**S** pulses at the midpoint.

the center of a free precession period (Figure 15). Once again for the vector picture, assume a chemical shift of zero for the **I** spin. The α and β labeled **I** vectors have different precession frequencies due to the local field of the α or β **S** spins. In this sequence, the time allowed for the first free precession period is set such that the vectors separate in phase by 90°. This value is $1/(4*J_{IS})$, where J_{IS} is the coupling constant between **I** and **S**. The 180° pulse applied to the **S** spin interchanges the α and β spin states of **S**. This inversion swaps the frequencies of the **I** vectors and direction of their precession reverses. The 180° $\mathbf{I_x}$ pulse rotates the **I** spin vectors to their mirror position in the XY plane. The precession due to coupling during t_2 brings the vectors into opposition along the X axis. This is identical to the antiphase state $\mathbf{I_xS_z}$ as described in Eqn. 7. In this analysis the **I** and **S** 180° pulses were treated sequentially. The same result is obtained if the pulses are simultaneous or swapped in time order, as long as the difference in time between the pulses is much smaller than $1/(4*J_{IS})$. Inclusion of both **I** and **S** 180° pulses at the midpoint allow coupling to continue to evolve. Had a time other than $n*1/(4*J_{IS})$been chosen, where n is an odd integer, the state would include both in-phase $\mathbf{I_y}$ and antiphase $\mathbf{I_xS_z}$ coherence. Choosing n*1/(2*J) would yield pure in-phase $\mathbf{I_y}$ coherence.

Equation 36 shows the sequence of rotations for this pulse sequence.

$$\xrightarrow{\pi/2\hat{I}_x} \xrightarrow{\omega_S t_1 \hat{S}_z} \xrightarrow{\omega_I t_1 \hat{I}_z} \xrightarrow{\pi J_{IS} t_1 \widehat{I_z S_z}} \xrightarrow{\pi \hat{I}_x} \xrightarrow{\pi \hat{S}_x} \xrightarrow{\pi J_{IS} t_2 \widehat{I_z S_z}} \xrightarrow{\omega_I t_2 \hat{I}_z} \xrightarrow{\omega_S t_2 \hat{S}_z} \tag{36}$$

Introducing an identity $-\pi\hat{S}_x\pi\hat{S}_x$ one obtains Eqn. 37.

$$\xrightarrow{\pi/2\widehat{I_x}}\xrightarrow{\omega_S t_1\widehat{S_z}}\xrightarrow{\omega_I t_1\widehat{I_z}}\xrightarrow{\pi J_{IS}t_1\widehat{I_zS_z}}\xrightarrow{\pi\widehat{I_x}}$$
$$\left[\xrightarrow{\pi\widehat{S_x}}\xrightarrow{\pi J_{IS}t_2\widehat{I_zS_z}}\xrightarrow{-\pi\widehat{S_x}}\right]\xrightarrow{\pi\widehat{S_x}} \qquad (37)$$
$$\xrightarrow{\omega_I t_2\widehat{I_z}}\xrightarrow{\omega_S t_2\widehat{S_z}}$$

Simplifying the bracketed terms in Eqn. 37 and introducing $-\pi\widehat{I_x}\pi\widehat{I_x}$, Eqn. 38 is obtained.

$$\xrightarrow{\pi/2\widehat{I_x}}\xrightarrow{\omega_S t_1\widehat{S_z}}\xrightarrow{\omega_I t_1\widehat{I_z}}\xrightarrow{\pi J_{IS}t_1\widehat{I_zS_z}}$$
$$\left[\xrightarrow{\pi\widehat{I_x}}\xrightarrow{-\pi J_{IS}t_2\widehat{I_zS_z}}\xrightarrow{-\pi\widehat{I_x}}\right]\xrightarrow{\pi\widehat{I_x}}\xrightarrow{\pi\widehat{S_x}} \qquad (38)$$
$$\xrightarrow{\omega_I t_2\widehat{I_z}}\xrightarrow{\omega_S t_2\widehat{S_z}}$$

Simplifying the bracketed terms gives Eqn. 39.

$$\xrightarrow{\pi/2\widehat{I_x}}\xrightarrow{\omega_S t_1\widehat{S_z}}\xrightarrow{\omega_I t_1\widehat{I_z}}\xrightarrow{\pi J_{IS}t_1\widehat{I_zS_z}}\xrightarrow{\pi J_{IS}t_2\widehat{I_zS_z}}$$
$$\xrightarrow{\pi\widehat{I_x}}\xrightarrow{\pi\widehat{S_x}}\xrightarrow{\omega_I t_2\widehat{I_z}}\xrightarrow{\omega_S t_2\widehat{S_z}} \qquad (39)$$

Combining the adjacent $\pi J_{IS}t\widehat{I_zS_z}$ terms gives Eqn. 40.

$$\xrightarrow{\pi/2\widehat{I_x}}\xrightarrow{\pi J_{IS}(t_1+t_2)\widehat{I_zS_z}}\xrightarrow{\omega_S t_1\widehat{S_z}}\xrightarrow{\pi\widehat{S_x}}\xrightarrow{\omega_S t_2\widehat{S_z}}$$
$$\xrightarrow{\omega_I t_1\widehat{I_z}}\xrightarrow{\pi\widehat{I_x}}\xrightarrow{\omega_I t_2\widehat{I_z}} \qquad (40)$$

Removing the chemical shift terms by introducing π rotation identities and simplifying as above with $t_1=t_2=t$, Eqn. 41 is obtained.

$$\xrightarrow{\pi/2\widehat{I_x}}\xrightarrow{\pi J_{IS}t\widehat{I_zS_z}}\xrightarrow{\pi\widehat{S_x}}\xrightarrow{\pi\widehat{I_x}} \qquad (41)$$

The simultaneous π pulses on **I** and **S** in the center of the spin echo eliminates the chemical shift for both **I** and **S** spins and allows scalar coupling to evolve for the entire period.

To recapitulate, there is one case of pulse-interrupted free precession for an isolated spin system **I** and there are 3 cases for an **I-S** coupled spin system. Below are a set of rules for these cases, including the case of free precession without any pulse interruptions. These rules are general in that they do not depend on the state of the **I** or **S** spin that enters the period. As a simplification, the absolute phase of the coherences at the end of the pulse-interrupted free precession period is not included these rules. In situations where the phase is important, Eqns. 18, 29, 35, 41 contain the required rotations. The phase for an isolated spin can be determined from Eqn. 17.

1) Isolated spin **I**: no pulses during the free precession period
    a. The chemical shift (and magnetic field inhomogeneities) of the **I** spin evolves for the full period
2) Isolated spin **I**: A π**I** pulse at the midpoint of the free precession period
    a. No net chemical shift evolution of **I** for the free precession period
3) Coupled **IS** spin system: no pulses during the free precession period
    a. The chemical shifts (and magnetic field inhomogeneities) of the **I** and **S** spins evolve for the full period
    b. Coupling evolves for the full period
4) Coupled **IS** spin system: a π**I** pulse at the midpoint of the free precession period
    a. No net chemical shift evolution of **I** for the free precession period
    b. The chemical shift of **S** evolves for the full period
    c. No net coupling at the end of the period; the system is decoupled

5) Coupled **IS** spin system: a π**S** pulse at the midpoint of the free precession period
    a. The chemical shift of **I** evolves for the full period
    b. No net chemical shift evolution of **S** for the free precession period
    c. No net coupling at the end of the period; the system is decoupled
6) Coupled **IS** spin system: Simultaneous π**I** and π**S** pulses at the midpoint of the free precession period
    a. No net chemical shift evolution of **I** or **S** for the free precession period
    b. Coupling evolves for the full period

With these rules in hand, it becomes straightforward to determine the behavior of many pulse sequences by inspection.

Decoupling

Consider a simple application of these rules in the experiment where there is a coupled spin system but during acquisition decoupling is applied. This is a normal situation when observing ^{13}C spectra. The multiplets due to coupling to ^{1}H spins are usually suppressed by decoupling. Figure 16 is a (naïve) approach to decoupling a coupled spin system

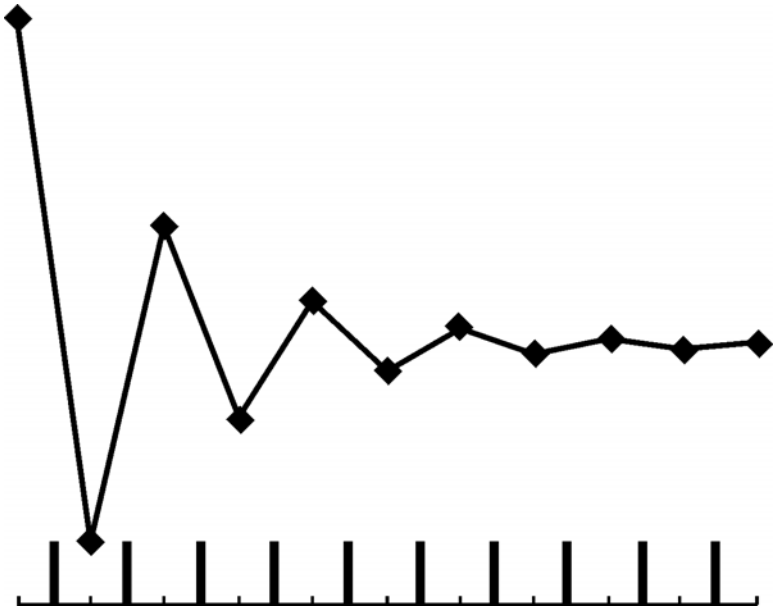

Figure 16. Example of a possible (but not very good) method for decoupling. The diamonds are the data points that are digitized in the NMR receiver. The pulses at the bottom are π rotations on the coupled nuclei placed at the midpoint of the data samples.

during acquisition. The detected NMR signal (free induction decay) is represented as the solid line and the diamonds are the sampling points. No pulses are applied to the detected signal during acquisition. The pulses at the bottom represent π pulses on the coupled spin placed at the midpoint of the sampling delay. This is identical to a free precession period for an **I** spin with a **πS** pulse applied at the midpoint of the period. Since the only data points that are sampled are at the end of the period, Eqn. 35 shows that the detected signal has no coupling information. The **I** signal is decoupled from the **S** spin. This is not a very good decoupling sequence in practice, the power dissipated from the rapid **πI** pulses will likely boil the sample and probably cause damage to the NMR probe. This is, however, a very common method for decoupling during the chemical shift labeling periods, t_1, in the indirect dimensions of multidimensional NMR. Only one pulse is applied since only one data point is collected per t_1 point and therefore there is not a problem with power dissipation.

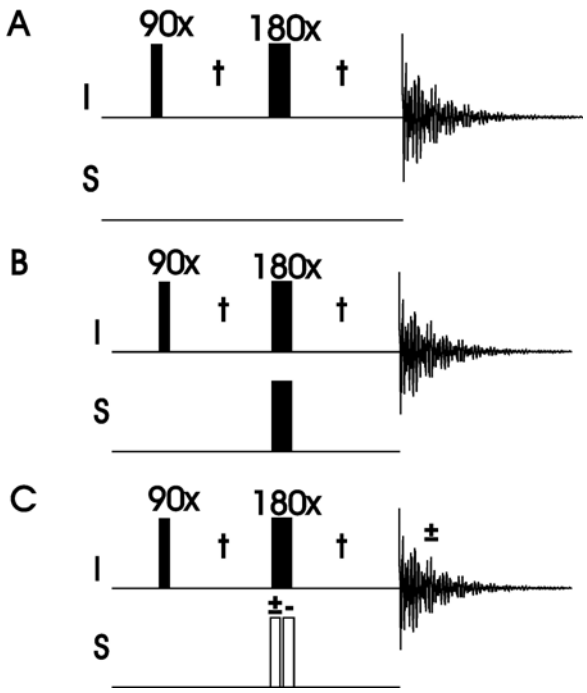

Figure 17. Pulse sequences used to edit coupled spins from uncoupled spins. Sequences A and B were discussed above. Sequence C is a typical implementation that combines experiments A and B. The S π pulse is split into two π/2 pulses and the phase of one is inverted every other acquisition along with inverting the receiver phase.

Spectral editing

As another example of the use of these pulse-interrupted free precession sequences, consider a large molecule with only one atom substituted with 100 % ^{13}C. The remaining carbon atoms have the natural abundance of ^{13}C (1%) and will be ignored in this discussion. A ^{1}H-^{13}C editing sequence can be designed to resolve the single ^{1}H-^{13}C in the

presence of a large number of ^{1}H-^{12}C resonances. By combining the results of the pulse sequences shown in Fig. 17, we can separate the protons that are isolated (^{1}H-^{12}C) from those that are coupled (^{1}H-^{13}C). The composite rotation for Fig. 17A is contained in Eqn. 42 and that for Fig. 17B is in Eqn. 43. In this experiment, the phases of the coherences are important, so all of the rotation operators in the composite rotations will be included.

$$\xrightarrow{3\pi/2\widehat{I_x}} \xrightarrow{\omega_S(2t)\widehat{S_z}} \tag{42}$$

$$\xrightarrow{\pi/2\widehat{I_x}} \xrightarrow{\pi J_{IS}\,2t\widehat{I_zS_z}} \xrightarrow{\pi\widehat{S_x}} \xrightarrow{\pi\widehat{I_x}} \tag{43}$$

For an isolated spin, the coupling operator in Eqn. 43 does not affect the behavior of the **I** spin in the free precession period since there is no **S** coupling partner. The product operator computation of Eqns. 42 and 43 for an isolated spin **I** (^{1}H-^{12}C) and a coupled **IS** spin system (^{1}H-^{13}C) is given in Table 2.

Table 2. Calculation of an isolated and coupled spin system subjected to the pulse sequences in Figs. 17A and 17B

1	**^{1}H-^{12}C**	$I_z \xrightarrow{3\pi/2\widehat{S_x}} I_y \xrightarrow{\omega_S(2t)\widehat{S_z}} I_y$
2	**^{1}H-^{12}C**	$I_z \xrightarrow{\pi/2\widehat{I_x}} -I_y \xrightarrow{\pi J_{IS}t\widehat{I_zS_z}} -I_y \xrightarrow{\pi\widehat{S_x}} -I_y \xrightarrow{\pi\widehat{I_x}} I_y$
3	**^{1}H-^{13}C**	$I_z \xrightarrow{3\pi/2\widehat{S_x}} I_y \xrightarrow{\omega_S(2t)\widehat{S_z}} I_y$
4	**^{1}H-^{13}C**	$I_z \xrightarrow{\pi/2\widehat{I_x}} -I_y \xrightarrow{\pi J_{IS}\,2t\widehat{I_zS_z}} -I_y\cos(\pi J_{IS}\,2t) + I_xS_z\sin(\pi J_{IS}\,2t)$ $\xrightarrow{\pi\widehat{S_x}} -I_y\cos(\pi J_{IS}\,2t) - I_xS_z\sin(\pi J_{IS}\,2t)$ $\xrightarrow{\pi\widehat{I_x}} I_y\cos(\pi J_{IS}\,2t) - I_xS_z\sin(\pi J_{IS}\,2t)$

The response of the isolated spin to both sequences is identical. Both sequences leave the spin in the $\mathbf{I_y}$ state. If the free precession time **t** is set to $1/2J_{IS}$ giving a total time of $1/J_{IS}$, the equation in line 4 of Table 2 simplifies to $\mathbf{-I_y}$. For the coupled spin system, the phase is inverted relative to the experiment in line 3. In order to combine the two spectra from the coupled spin system, the data sets must be subtracted. This will eliminate the signals from the isolated spin, since the phase is the same in the two experiments. Figure 17C shows a typical implementation of this experiment. In this experiment the $\pi\mathbf{S}$ pulse is broken into two $\pi/2$ pulses. In the odd numbered acquisitions the phase of the two $\pi/2$ pulses are the same and therefore the total rotation of **S** is by π. The data is summed to memory. In the even numbered acquisitions, the phase of one of the $\pi/2$ pulses is inverted making the total rotation 0. This essentially removes any pulse on the **S** channel. The data from this experiment is subtracted from the data of the odd numbered acquisitions.

Coherence transfer: INEPT

The INEPT sequence. **S** chemical shift terms are ignored. If chemical shift existed it would be eliminated by the $\xrightarrow{\pi\widehat{S_x}}$ term.

$$\xrightarrow{\pi/2\widehat{I_x}} \xrightarrow{\omega_I t\widehat{I_z}} \xrightarrow{\pi/4\widehat{I_zS_z}}$$

$$\xrightarrow{\pi\widehat{I_x}} \xrightarrow{\pi\widehat{S_x}} \xrightarrow{\pi/4\widehat{I_zS_z}}$$

$$\xrightarrow{\omega_I t\widehat{I_z}} \xrightarrow{\pi/2\widehat{I_y}} \xrightarrow{\pi/2\widehat{S_x}}$$

As above in the simultaneous **I** and **S** 180° pulse calculation, π identities are introduced for both **I** and **S** spins.

$$\xrightarrow{\pi/2\widehat{I_x}} \xrightarrow{\omega_I t\widehat{I_z}}$$

$$\xrightarrow{\pi\widehat{S_x}} \xrightarrow{-\pi\widehat{S_x}}$$

$$\xrightarrow{\pi\widehat{I_x}} \xrightarrow{-\pi\widehat{I_x}}$$

$$\xrightarrow{\pi/4\widehat{I_zS_z}} \xrightarrow{\pi\widehat{I_x}} \xrightarrow{\pi\widehat{S_x}}$$

$$\xrightarrow{\pi/4\widehat{I_zS_z}} \xrightarrow{\omega_I t\widehat{I_z}} \xrightarrow{\pi/2\widehat{I_y}} \xrightarrow{\pi/2\widehat{S_x}}$$

Simplifying the coupling term as above.

$$\xrightarrow{\pi/2\widehat{I_x}} \xrightarrow{\omega_I t\widehat{I_z}}$$

$$\xrightarrow{\pi\widehat{S_x}} \xrightarrow{\pi\widehat{I_x}}$$

$$\xrightarrow{\pi/2\widehat{I_zS_z}}$$

$$\xrightarrow{\omega_I t\widehat{I_z}} \xrightarrow{\pi/2\widehat{I_y}} \xrightarrow{\pi/2\widehat{S_x}}$$

Removing the I chemical shift terms,

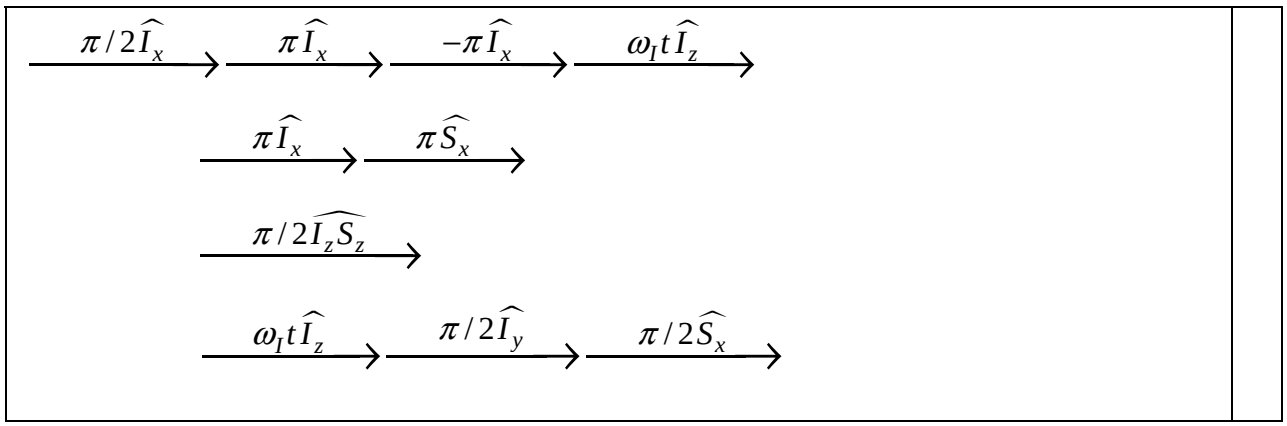

One obtains

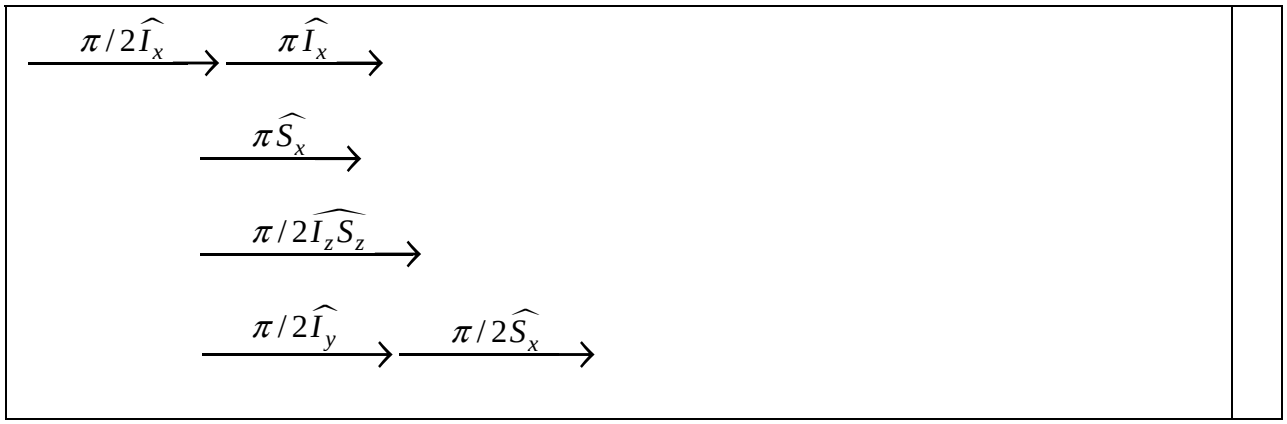

We can further simplify the sequence by introducing π/2 rotation identities.

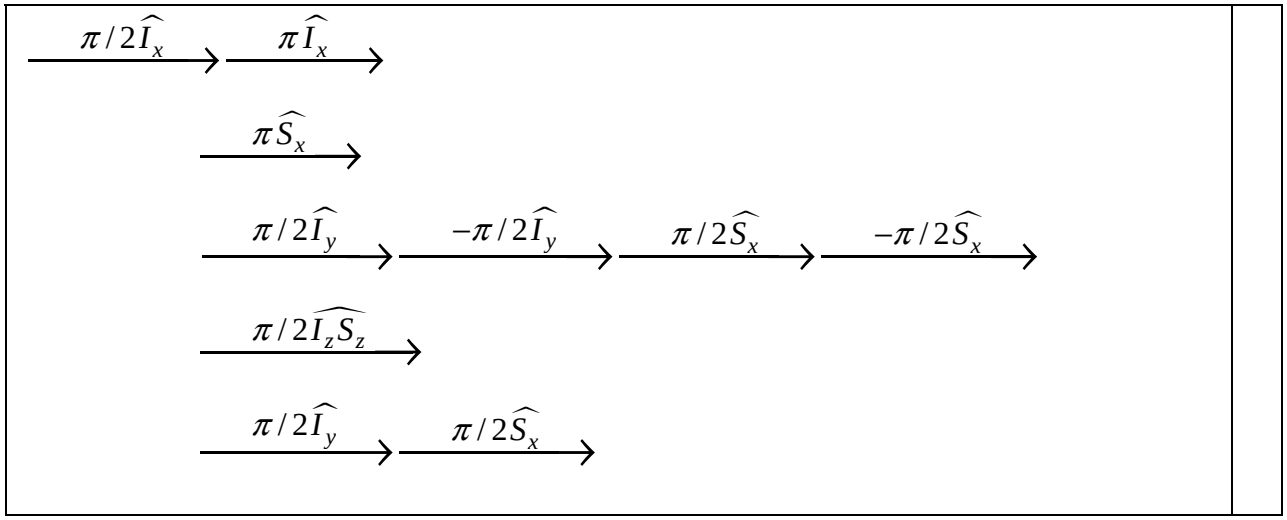

Rotating the $\xrightarrow{\pi J_{IS} t\widehat{I_z S_z}}$ term by the $\xrightarrow{\pi/2\widehat{I_y}}$ $\xrightarrow{\pi/2\widehat{S_x}}$ terms.

$$\xrightarrow{\pi/2\widehat{I_x}} \xrightarrow{\pi\widehat{I_x}}$$

$$\xrightarrow{\pi\widehat{S_x}}$$

$$\xrightarrow{\pi/2\widehat{I_y}} \xrightarrow{\pi/2\widehat{S_x}}$$

$$\xrightarrow{-\pi/2\widehat{I_xS_y}}$$

Simplifying.

$$\xrightarrow{3\pi/2\widehat{I_x}} \xrightarrow{\pi/2\widehat{I_y}}$$

$$\xrightarrow{3\pi/2\widehat{S_x}}$$

$$\xrightarrow{-\pi/2\widehat{I_xS_y}}$$

Calculation starting from $\mathbf{I_z}$.

$$I_z \xrightarrow{3\pi/2\widehat{I_x}} I_y \xrightarrow{\pi/2\widehat{I_y}} I_y$$

$$\xrightarrow{3\pi/2\widehat{S_x}} I_y$$

$$\xrightarrow{-\pi/2\widehat{I_xS_y}} I_zS_y$$

Calculation starting from $\mathbf{I_x}$.

$$I_x \xrightarrow{3\pi/2\widehat{I_x}} I_x \xrightarrow{\pi/2\widehat{I_y}} -I_z$$

$$\xrightarrow{3\pi/2\widehat{S_x}} -I_z$$

$$\xrightarrow{-\pi/2\widehat{I_x S_y}} I_y S_y$$

Refocused INEPT

$$\xrightarrow{\pi/2\widehat{I_x}} \xrightarrow{\omega_I t\widehat{I_z}} \xrightarrow{\pi/4\widehat{I_zS_z}}$$

$$\xrightarrow{\pi\widehat{I_x}} \xrightarrow{\pi\widehat{S_x}} \xrightarrow{\pi/4\widehat{I_zS_z}}$$

$$\xrightarrow{\omega_I t\widehat{I_z}} \xrightarrow{\pi/2\widehat{I_y}} \xrightarrow{\pi/2\widehat{S_x}}$$

$$\xrightarrow{\omega_S t\widehat{S_z}} \xrightarrow{\pi/4\widehat{I_zS_z}}$$

$$\xrightarrow{\pi\widehat{I_x}} \xrightarrow{\pi\widehat{S_x}}$$

$$\xrightarrow{\omega_S t\widehat{S_z}} \xrightarrow{\pi/4\widehat{I_zS_z}}$$

Simplifying the INEPT.

$$\xrightarrow{3\pi/2\widehat{I_x}} \xrightarrow{\pi/2\widehat{I_y}}$$

$$\xrightarrow{3\pi/2\widehat{S_x}}$$

$$\xrightarrow{-\pi/2\widehat{I_xS_y}}$$

$$\xrightarrow{\omega_S t\widehat{S_z}} \xrightarrow{\pi/4\widehat{I_zS_z}}$$

$$\xrightarrow{\pi\widehat{I_x}} \xrightarrow{\pi\widehat{S_x}}$$

$$\xrightarrow{\omega_S t\widehat{S_z}} \xrightarrow{\pi/4\widehat{I_zS_z}}$$

The refocusing part is simplified using the same techniques

$$\xrightarrow{3\pi/2\widehat{I_x}} \xrightarrow{\pi/2\widehat{I_y}}$$

$$\xrightarrow{3\pi/2\widehat{S_x}}$$

$$\xrightarrow{-\pi/2\widehat{I_xS_y}}$$

$$\xrightarrow{\pi\widehat{I_x}} \xrightarrow{\pi\widehat{S_x}}$$

$$\xrightarrow{\pi/2\widehat{I_zS_z}}$$

Starting from Iz:

$$I_z \xrightarrow{3\pi/2\widehat{I_x}} I_y \xrightarrow{\pi/2\widehat{I_y}} I_y$$

$$\xrightarrow{3\pi/2\widehat{S_x}} I_y$$

$$\xrightarrow{-\pi/2\widehat{I_xS_y}} -I_zS_y$$

$$\xrightarrow{\pi\widehat{I_x}} I_zS_y \xrightarrow{\pi\widehat{S_x}} -I_zS_y$$

$$\xrightarrow{\pi/2\widehat{I_zS_z}} S_x$$

INEPT-reverse INEPT (Editing)

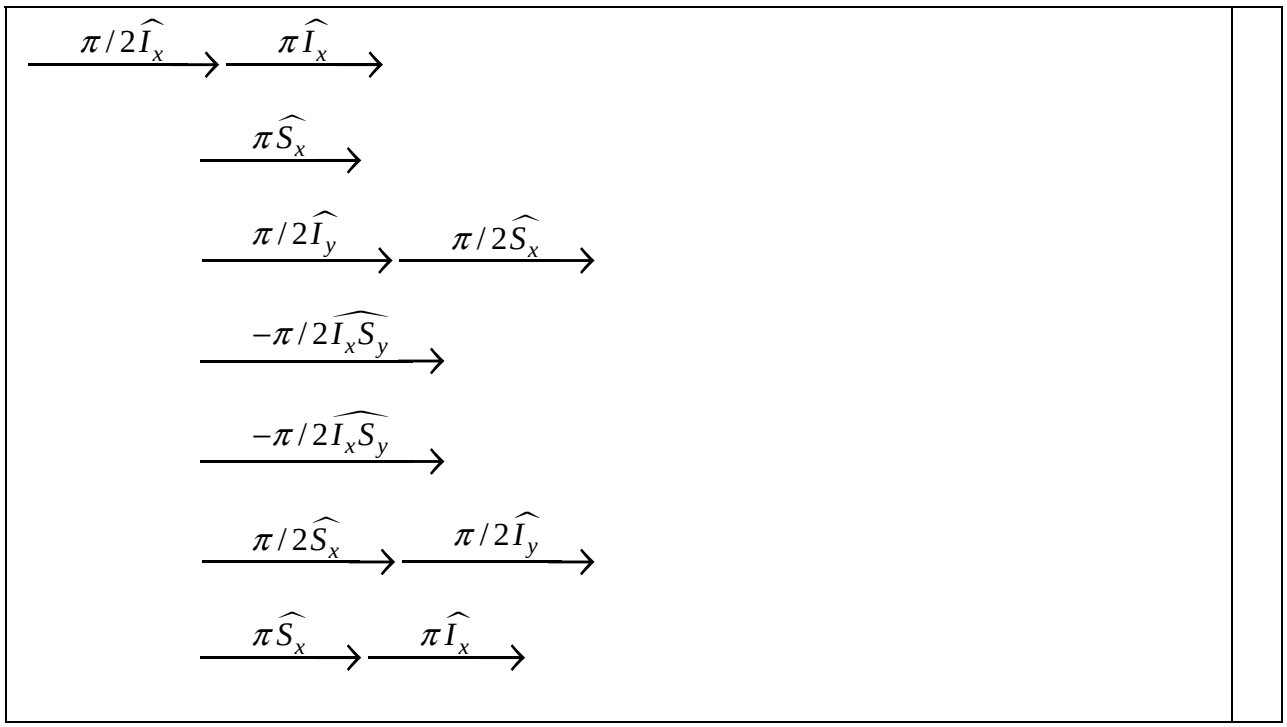

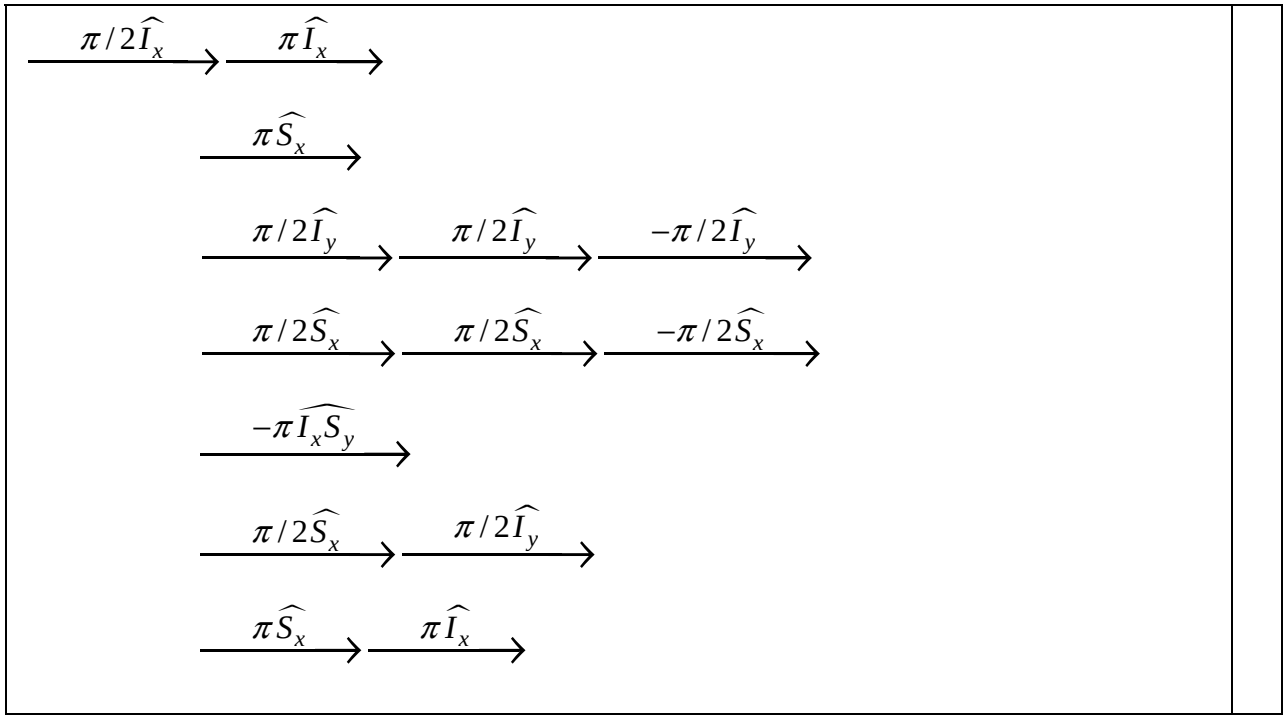

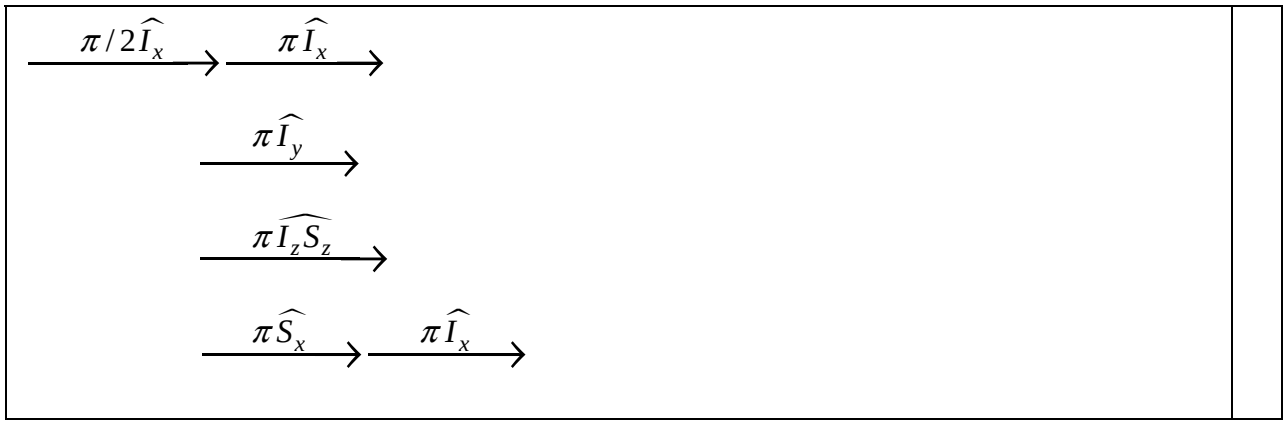
$\pi/2\widehat{I_x}$
$\pi\widehat{I_x}$
$\pi\widehat{I_y}$
$\pi\widehat{I_z S_z}$
$\pi\widehat{S_x}$
$\pi\widehat{I_x}$

HSQC-Heteronuclear Single Quantum Correlation (coupled)

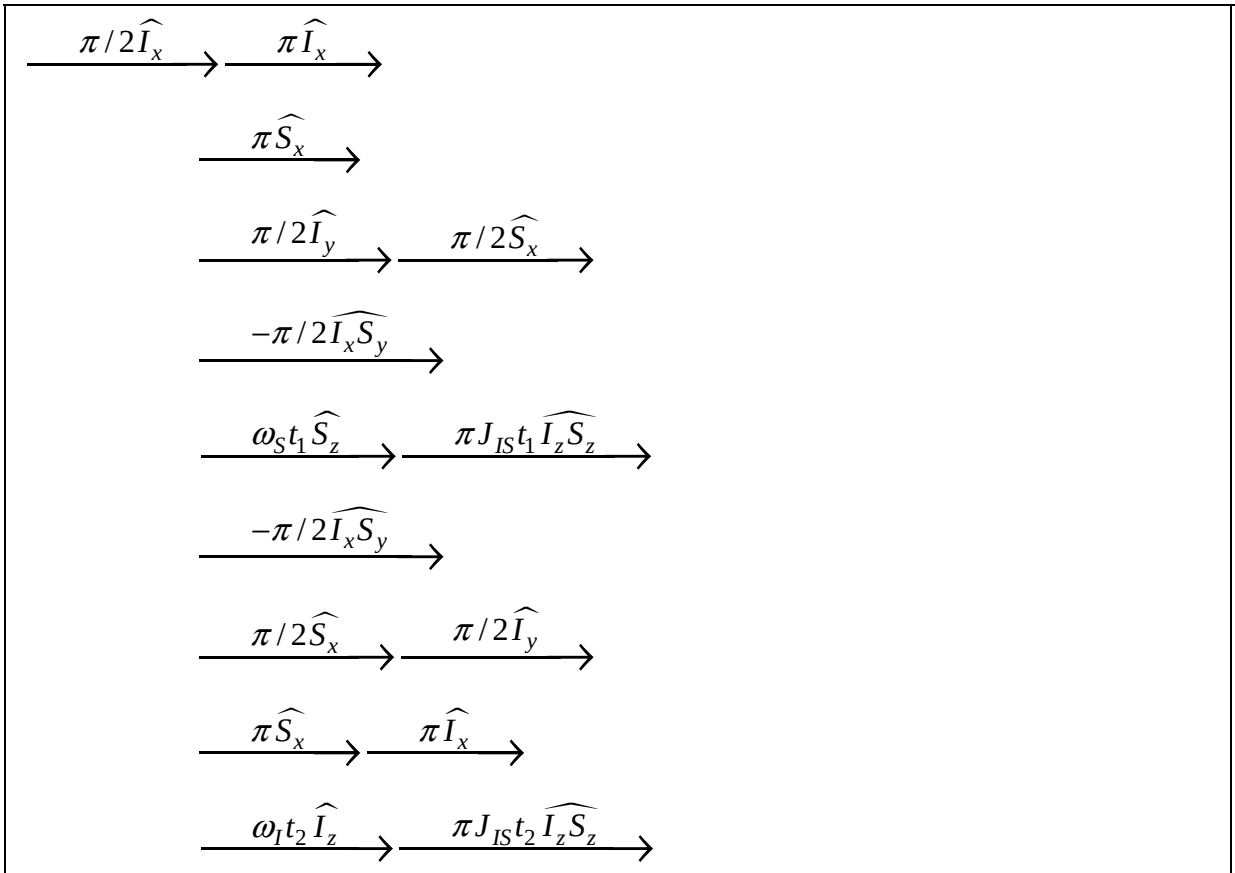

HSQC-Heteronuclear Single Quantum Correlation (decoupled)

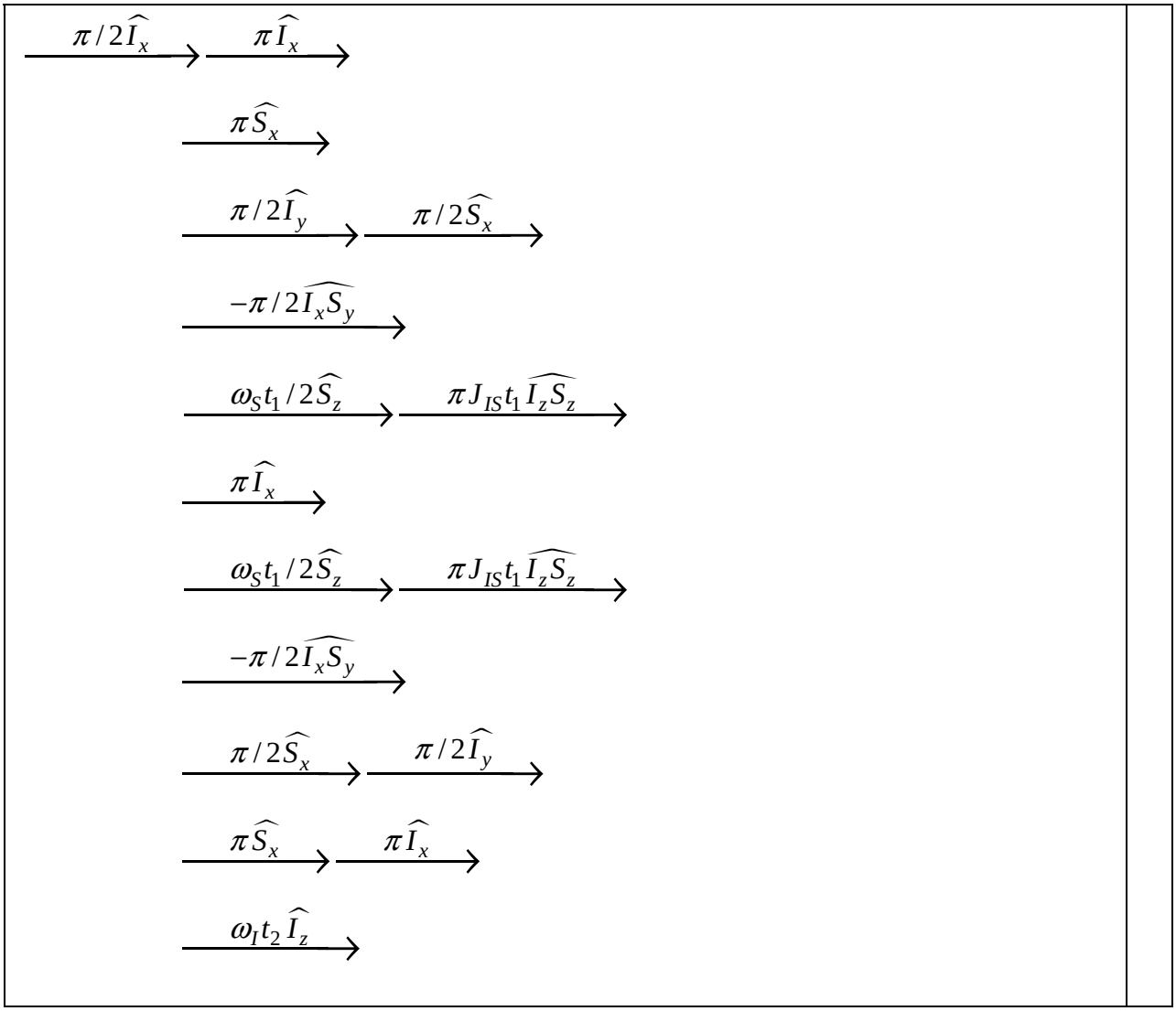

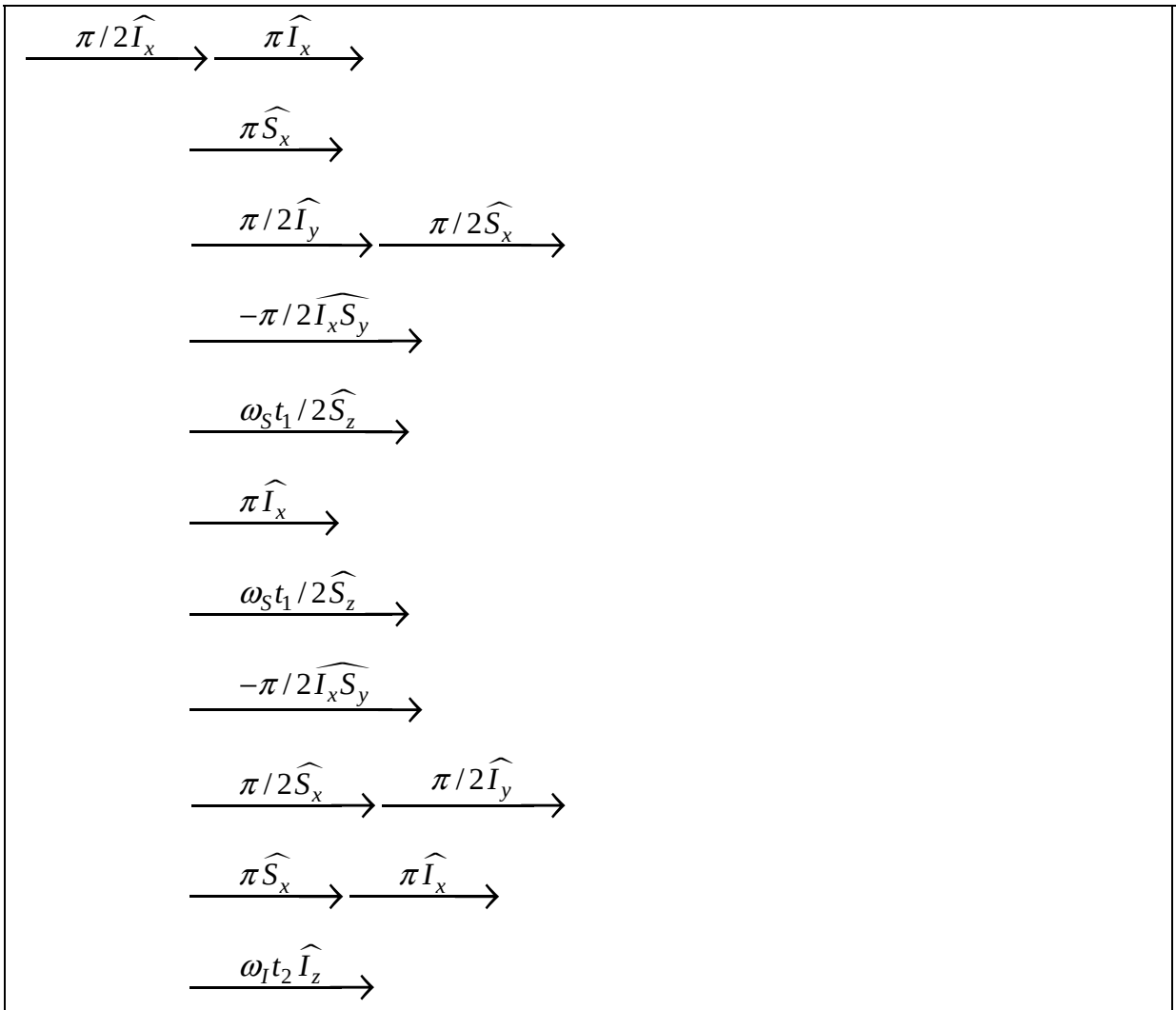
$\pi/2\widehat{I_x}$
$\pi\widehat{I_x}$
$\pi\widehat{S_x}$
$\pi/2\widehat{I_y}$
$\pi/2\widehat{S_x}$
$-\pi/2\widehat{I_xS_y}$
$\omega_S t_1/2\widehat{S_z}$
$\pi\widehat{I_x}$
$\omega_S t_1/2\widehat{S_z}$
$-\pi/2\widehat{I_xS_y}$
$\pi/2\widehat{S_x}$
$\pi/2\widehat{I_y}$
$\pi\widehat{S_x}$
$\pi\widehat{I_x}$
$\omega_I t_2\widehat{I_z}$

Filtered

$\xrightarrow{\pi/2\widehat{I_x}} \xrightarrow{\omega_I t\widehat{I_z}} \xrightarrow{\pi J_{IS} t\widehat{I_z S_z}}$ $\xrightarrow{\pi\widehat{S_x}} \xrightarrow{\pi\widehat{I_x}}$ $\xrightarrow{\omega_I t\widehat{I_z}} \xrightarrow{\pi J_{IS} t\widehat{I_z S_z}}$ $\xrightarrow{\pi/2\widehat{I_x}} \xrightarrow{\pi/2\widehat{S_x}}$	

$\xrightarrow{\pi/2\widehat{I_x}} \xrightarrow{\pi\widehat{S_x}} \xrightarrow{\pi\widehat{I_x}}$ $\xrightarrow{\pi/2\widehat{I_x}} \xrightarrow{-\pi/2\widehat{I_x}}$ $\xrightarrow{\pi/2\widehat{S_x}} \xrightarrow{-\pi/2\widehat{S_x}}$ $\xrightarrow{\pi J_{IS} 2t\widehat{I_z S_z}}$ $\xrightarrow{\pi/2\widehat{I_x}} \xrightarrow{\pi/2\widehat{S_x}}$	

$\xrightarrow{\pi/2\widehat{I_x}} \xrightarrow{\pi\widehat{S_x}} \xrightarrow{\pi\widehat{I_x}}$ $\xrightarrow{\pi/2\widehat{I_x}} \xrightarrow{\pi/2\widehat{S_x}}$ $\xrightarrow{\pi J_{IS} 2t\widehat{I_y S_y}}$	

$I_z \xrightarrow{\pi/2\widehat{I_x}} -I_y \xrightarrow{\pi\widehat{S_x}} -I_y \xrightarrow{\pi\widehat{I_x}} I_y$ $\xrightarrow{\pi/2\widehat{I_x}} I_z \xrightarrow{\pi/2\widehat{S_x}} I_z$ $\xrightarrow{\pi J_{IS} 2t\widehat{I_y S_y}} I_x S_y$	

Appendix A. Algorithmic approach to commutators

The 3 dimensional axes that are used to describe the rotations of the product operators are obtained through the use of the commutation rules for angular momentum. Equation A1 and its cyclic permutations are the basic angular momentum commutators.

$$\left[I_x, I_y \right] = I_x * I_y - I_y * I_x = iI_z \tag{A1}$$

If the cyclic order is changed by one interchange, then the result is negated. These commutation relationships can be shown easily through multiplications of the Pauli matrices (Eqn A2).

$$\underset{I_E}{\begin{bmatrix} 1 & 0 \\ 0 & 1 \end{bmatrix}} \quad \underset{I_x}{\begin{bmatrix} 0 & 1/2 \\ 1/2 & 0 \end{bmatrix}} \quad \underset{I_y}{\begin{bmatrix} 0 & -i/2 \\ i/2 & 0 \end{bmatrix}} \quad \underset{I_z}{\begin{bmatrix} 1/2 & 0 \\ 0 & -1/2 \end{bmatrix}} \tag{A2}$$

The Pauli matrices are the density matrices for a single isolated spin. Equation A1 can be calculated as in Eqn. A3.

$$\underset{I_x * I_y}{\begin{bmatrix} 0 & 1/2 \\ 1/2 & 0 \end{bmatrix} * \begin{bmatrix} 0 & -i/2 \\ i/2 & 0 \end{bmatrix}} - \underset{I_y * I_x}{\begin{bmatrix} 0 & -i/2 \\ i/2 & 0 \end{bmatrix} * \begin{bmatrix} 0 & 1/2 \\ 1/2 & 0 \end{bmatrix}} \tag{A3}$$

$$\begin{bmatrix} i/4 & 0 \\ 0 & -i/4 \end{bmatrix} - \begin{bmatrix} -i/4 & 0 \\ 0 & i/4 \end{bmatrix} = i * \underset{iI_z}{\begin{bmatrix} 1/2 & 0 \\ 0 & 1/2 \end{bmatrix}}$$

Kronecker products for coupled spins can be generated by the matrix operation in Eqn A4, which

shows the method for determining the density matrix of $\mathbf{I_xS_z}$.

$$
\begin{aligned}
I_x \otimes S_z &= \begin{bmatrix} I_x^{11}S_z & I_x^{12}S_z \\ I_x^{21}S_z & I_x^{22}S_z \end{bmatrix} \\
&= \begin{bmatrix} 0*\begin{bmatrix} 1/2 & 0 \\ 0 & -1/2 \end{bmatrix} & 1/2*\begin{bmatrix} 1/2 & 0 \\ 0 & -1/2 \end{bmatrix} \\ 1/2*\begin{bmatrix} 1/2 & 0 \\ 0 & -1/2 \end{bmatrix} & 0*\begin{bmatrix} 1/2 & 0 \\ 0 & -1/2 \end{bmatrix} \end{bmatrix} \\
&= \begin{bmatrix} 0 & 0 & 1/4 & 0 \\ 0 & 0 & 0 & -1/4 \\ 1/4 & 0 & 0 & 0 \\ 0 & -1/4 & 0 & 0 \end{bmatrix}
\end{aligned}
\tag{A4}
$$

There are a number of other more complex commutators that can be derived from Eqn. A1-A3, but there is a simple algorithmic approach to constructing the angular momentum commutation rules. The following algorithm starts from knowledge of two operators, here the state spin operator (the vector to be rotated) and the rotation operator. This algorithm constructs the label for the third axis of a 3-dimensional coordinate system (the commutator) that is consistent with the angular momentum commutation rules for this rotation or indicates that the operators commute and that a three dimensional coordinate system is not possible.

Only bilinear operators are allowed.

Active spins

Passive spins

I. Need to generate a right-handed **xyz** triplet for one (and only one) spin.

II. One axis must be a X, Y, or Z operator. No three dimensional axis system is possible where all three axis are labeled with a product of two operators unless the other operator is a passive spin.

III. The other two axes must be interchangeable by the X, Y, or Z rotation.

Example 1:

State_1 = $\mathbf{I_zS_x}$ *State_2* = $\mathbf{I_zS_z}$

$\mathbf{I_zS_z}$ can be rotated into $\mathbf{I_zS_x}$ by a rotation about $\mathbf{S_y}$**.**

The proper right-handed coordinate system is shown in Figure A1.

Example 2:

State_1 = $\mathbf{I_x}$ *State_2* = $\mathbf{I_yS_x}$

Ix rotates IySx into IzSx.

The proper right-handed coordinate system is shown in Figure A2.

Example 3:

State_1 = $\mathbf{I_z}$ *State_2* = $\mathbf{I_zS_z}$

Iz is parallel to the Iz term in IzSz. No rotation can take place and there is no possible coordinate system.

Example 4:

State_1 = $\mathbf{I_xS_y}$ *State_2* = $\mathbf{I_zS_z}$

No single X, Y, or Z rotation can rotate IxSy into IzSz. No coordinate axis system can be drawn.

Example 5:

State_1 = $\mathbf{I_zS_xT_x}$ *State_2* = $\mathbf{I_zS_z}$

The T spin is passive. IzSz can be rotated into IzSx by Sy. The third state is SyTx.

Appendix B Equivalent rotations.

Equation B1 represents a series of rotations that are to be simplified. The general feature of this sequence is a rotation operator surrounded by two identical but opposite rotations.

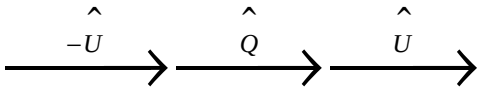	(B1)

This series of operators can be simplified by rotation of the central operator by the rightmost operator using the standard rules for rotations (Eqn. B2).

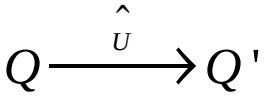	(B2)

The equivalent, simplified rotation operator to that series in Eqn. B1 is given in Eqn B3.

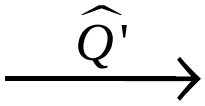	(B3)

This can be proven mathematically by a series expansion the unitary transforms (Eqn. B4).

This equivalence could also be shown through the use of matrices as in paper 1 of this series.

$$\xrightarrow{-\hat{U}} \xrightarrow{\hat{A}} \xrightarrow{\hat{U}}$$

$$\xrightarrow{\hat{A}} = e^{\mathrm{i}\phi \mathrm{A}} = \mathbf{1} + i\phi A + \frac{(i\phi)^2}{2!} A^2 + \cdots$$

$$\xrightarrow{-\hat{U}} = \hat{U}^{-1}$$

$$\hat{U}^{-1} e^{\mathrm{i}\phi \mathrm{A}} \hat{U} = \hat{U}^{-1} \left(\mathbf{1} + i\phi A + \frac{(i\phi)^2}{2!} A^2 + \cdots \right) \hat{U} \qquad \text{(B4)}$$

$$= \mathbf{1} + i\phi \hat{U}^{-1} A \hat{U} + \frac{(i\phi)^2}{2!} \hat{U}^{-1} A \hat{U} \hat{U}^{-1} A \hat{U} + \cdots$$

$$= \mathbf{1} + i\phi \hat{U}^{-1} A \hat{U} + \frac{(i\phi)^2}{2!} \left(\hat{U}^{-1} A \hat{U} \right)^2 + \cdots$$

$$= e^{\mathrm{i}\phi (\hat{U}^{-1} \mathrm{A} \hat{U})} = \xrightarrow{-\hat{U}} A \xrightarrow{\hat{U}}$$

(##).

As a concrete example, assume that in a series of rotation operators, the sequence in Eqn. B5 is found.

$$\xrightarrow{-\pi/2 \hat{S}_x} \xrightarrow{\pi J t \hat{I}_z \hat{S}_z} \xrightarrow{\pi/2 \hat{S}_x} \qquad \text{(B5)}$$

The $\pi/2$ operators surrounding the central operator are opposites and therefore the total sequence can be simplified by rotating the central operator by the rightmost operator. Note that this operation is rotating rotation operators. It follows the same rules as for rotating spin operators. The original sequence of Eqn. B5 can be substituted with Eqn. B6.

$$\xrightarrow{-\pi Jt\widehat{I_z S_y}} \tag{B6}$$

This procedure does not always give simple results (e.g. Eqn B7), but with judicious choices of the inserted identity operators, complicated sequences can be often simplified to a few simple rotations.

$$\xrightarrow{\pi/4\widehat{I_x}} \xrightarrow{wt\widehat{I_z}} \xrightarrow{-\pi/4\widehat{I_x}} = \xrightarrow{wt(\widehat{I_z}\cos(\pi/4)+\widehat{I_y}\sin(\pi/4))} \tag{B7}$$

$$\omega t * \begin{bmatrix} 1/2 & 1/\sqrt{2} & 1/2 \\ -1/\sqrt{2} & 0 & 1/\sqrt{2} \\ 1/2 & -1/\sqrt{2} & 1/2 \end{bmatrix} \tag{B8}$$

The composite rotation containing the non-commutating operators $\hat{\mathbf{I}}_z$ and $\hat{\mathbf{I}}_y$ does not simplify to an "easy" rotation operator around the X, Y, or Z axis (Eqn. B8). The rotation axis for this operator is along a vector that is 45° rotated from the Z axis in the YZ plane.